Anti-glioma effects of 2-aminothiophene-3-carboxamide derivatives, ANO1 channel blockers

Seunghye Choi, SeongShick Ryu, Kyoungmi Sim, Chiman Song, Injae Shin, Seong-Seop Kim, Young-Sun Lee, Jae-Yong Park, Taebo Sim

PII: S0223-5234(20)30660-7

DOI: https://doi.org/10.1016/j.ejmech.2020.112688

Reference: EJMECH 112688

To appear in: *European Journal of Medicinal Chemistry*

Received Date: 3 June 2020

Revised Date: 15 July 2020

Accepted Date: 21 July 2020

Please cite this article as: S. Choi, S. Ryu, K. Sim, C. Song, I. Shin, S.-S. Kim, Y.-S. Lee, J.-Y. Park, T. Sim, Anti-glioma effects of 2-aminothiophene-3-carboxamide derivatives, ANO1 channel blockers, *European Journal of Medicinal Chemistry*, https://doi.org/10.1016/j.ejmech.2020.112688.

ANO1 channel inhibition

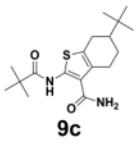

	ANO1 IC_{50} (μM)	
Assay Method	**9c**	**10q**
FLIPR format	3.10	2.36
Patch clamp	2.56	1.75

Migration and Invasion assay

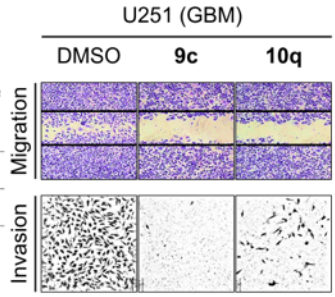

Synergistic effect on U251
9c and **TMZ**

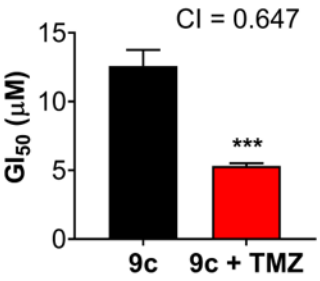

Anti-glioma effects of 2-aminothiophene-3-carboxamide derivatives, ANO1 channel blockers

Seunghye Choi[a,1] SeongShick Ryu[a,1], Kyoungmi Sim[b], Chiman Song[c,d], Injae Shin[a,e] Seong-Seop Kim[b], Young-Sun Lee[b], Jae-Yong Park[b] and Taebo Sim[a,c,e,*]

[a] KU-KIST Graduate School of Converging Science and Technology, Korea University, 145 Anam-ro, Seongbuk-gu, Seoul 02841, Republic of Korea.

[b] School of Biosystems and Biomedical Sciences, College of Health Sciences, Korea University, Seoul 02841, Republic of Korea.

[c] Chemical Kinomics Research Center, Korea Institute of Science and Technology, 5 Hwarangro 14-gil, Seongbuk-gu, Seoul 02792, Republic of Korea.

[d] Department of Agricultural Biotechnology, College of Agriculture and Life Sciences, Seoul National University, 1 Gwanak-ro, Gwanak-gu, Seoul 08826, Republic of Korea.

[e] Severance Biomedical Science Institute, Yonsei University College of Medicine, 50-1 Yonsei-ro, Seodaemun-gu, Seoul 03722, Republic of Korea.

[1] These authors are equally contributed to this work.

ABSTRACT

Anoctamin1 (ANO1), a calcium-activated chloride ion channel (CaCC), is associated with various physiological functions including cancer progression and metastasis/invasion. ANO1 has been considered as a promising target for cancer therapeutics as ANO1 is over-expressed in a variety of cancers including glioblastoma (GBM) and inhibition of ANO1 has been reported to suppress cell proliferation, migration and invasion in GBM. GBM is one of the most common and aggressive cancers with poor prognosis with median survival for 15 months. Lack of effective treatment options against GBM emphasizes urgent necessity of effective GBM therapeutics. In an effort to discover potent and selective ANO1 inhibitors capable of inhibiting GBM cells, we have designed and synthesized a series of new 2-aminothiophene-3-carboxamide derivatives and performed SAR studies using both fluorescent cellular membrane potential assay and whole-cell patch-clamp recording. We observed that among these substances, **9c** and **10q** strongly suppress ANO1 channel activities and possess remarkable selectivity over ANO2. Unique structural feature of **10q**, a cyclopentane-fused thiophene-3-carboxamide derivative, is the presence of benzoylthiourea functionality which dramatically contributes to activity. Both **9c** and **10q** suppress more strongly proliferation of GBM

cells than four reference compounds including **3**, Ani-9 and are also capable of inhibiting much more strongly colony formation than reference compounds in both 2D colony formation assay and 3D soft agar assay using U251 glioma cells. In addition, **9c** and **10q** suppress far more strongly migration/invasion of GBM cells than reference compounds. We, for the first time, found that the combination of ANO1 inhibitor (**9c** or **3**) and temozolomide (TMZ) brings about remarkable synergistic effects in suppressing proliferation of GBM cells. Our study may provide an insight into designing selective and potent ANO1 inhibitors aiming at GBM treatment.

Keywords: ANO1 chloride ion channel, ANO1 inhibitors, glioblastoma (GBM), 2-aminothiophene-3-carboxamides, combination of TMZ and ANO1 inhibitor

1. INTRODUCTION

Anotamin-1 (ANO1), a Ca^{2+}-activated chloride ion channel (CaCCs), plays important roles in cellular physiological processes including smooth muscle excitability, cardiac excitability and nociception, and epithelial secretion in various cell types[1, 2]. ANO1 has been considered as a promising target for targeted cancer therapeutics as ANO1 is amplified and over-expressed in various cancers such as breast[3], pancreas[4], prostate[5], urinary bladder[6], oesophagus[7], lung[8], head-and-neck squamous cell carcinoma (HNSCC)[9], gastrointestinal stromal tumors (GIST)[10], and glioblastoma (GBM)[11]. It has been reported that ANO1 is overexpressed in various GBM cells including U87MG[12], U138[13], and U251[14] and decrease of ANO1 expression by the treatment of siRNA suppresses proliferation[12], invasion and migration[14] of GBM cells. ANO2 (TMEM16B) has about ~60% sequence homology with ANO1 and is expressed in the cilia of olfactory sensory neurons[15] and mediates olfactory amplification[16]. Loss of ANO2 expression leads to markedly diminished action potential firing of inferior olivary neurons and ANO2 knockout mice exhibits severe cerebellar motor learning deficits[17]. It is therefore necessary to selectively inhibit ANO1 rather than ANO2 for anti-ANO1 drug discovery.

GBM is one of the most common and aggressive human cancers[18] and accouts for over 60% of malignant glioma. Only around 5% of GBM patients survive for 5 years. GBM cell invasion occurs in the parenchyma of the brain and surgical resection inevitably leads to recurrent disease[11]. Surgical resection followed by radiotherapy and concomitant and adjuvant chemotherapy with temozolomide (TMZ) has become the standard first-line therapy against GBM with a small increase (around 2.5 months) of the median survival[19]. Despite tremendous efforts to overcome GBM, effective therapeutics against GBM are still very limited. No standard treatment has been established for GBM recurrence which is almost inevitable and median survival is measured in months[20].

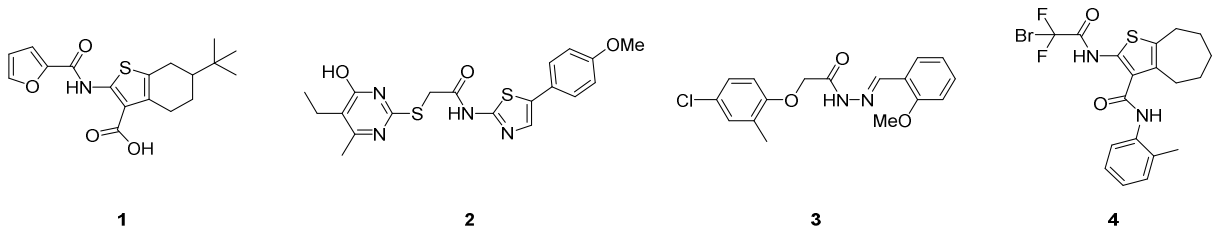

Figure 1. Representative ANO1 channel blockers

To date, a few small molecule inhibitors (Fig. 1) of ANO1 have been described including CaCCinh-A01 (**1**), T16Ainh-A01 (**2**), Ani-9 (**3**), and 10bm (**4**). Non-selective ANO1 ion channel blocker **1** (IC_{50} = 2.1 μM), a cyclohexa[*b*]thiophene derivative, is capable of decreasing ANO1 protein expression level by ER-associated proteasomal degradation, which causes appreciable suppressive effects on ANO1-dependent cellular proliferation in head and neck squamous cell carcinoma (HNSCC) and esophageal squamous cell carcinoma (ESCC) cells[21]. T16Ainh-A01 **2** (IC_{50} = 1.39 μM) discovered by high-throughput screening campaign inhibits the functional channel activity of ANO1 in vascular smooth muscle cells and relaxes human and mouse blood vessels[22].

Ani-9 (**3**), discovered from screening of 54,400 synthetic small molecules, is a selective and potent ANO1 inhibitor with an IC_{50} value of 77 nM[23]. Ani-9 (**3**), a benzylideneacetohydrazide derivative, has low metabolic stability with a half-life value of 32 minutes[24]. Another potent ANO1 inhibitor **4** belonging to one of the 2-acylaminocycloalkylthiophene-3-carboxylic acid arylamides (AACTs) has an IC_{50} value of 30 nM and displays over 10-fold improved metabolic stability compared with **3**[25]. As part of a program to perform GBM drug discovery, we have decided to explore effective ANO1 channel blockers and been interested in the AACT analogue **4**, the most potent ANO1 inhibitor although activity of **4** against GBM has not been reported. In an effort to discover potent and selective ANO1 inhibitors capable of inhibiting GBM cells, we have designed and synthesized a series of new 2-aminocycloalkylthiophene-3-carboxamide derivatives based on AACT analogue **4** and carried out an SAR study exploring inhibitory activities on GBM cells as well as against ANO1 ion channel. We observed that among the 33 synthetic 2-aminocycloalkylthiophene-3-carboxamide derivatives prepared for this SAR study, **9c** and **10q** completely block ANO1 channel activity with appreciable selectivity and significantly suppress proliferation and migration/invasion of GBM cells. Herein, we report that **9c** and **10q** are potent and selective ANO1 inhibitors as valuable hit compounds for GBM drug discovery.

2. RESULT AND DISCUSSION

2.1. Synthesis

All the 2-aminothiophene-3-carboxamide derivatives were synthesized in a very straightforward manner as described in Scheme 1. In order to obtain C-4 and C-5 unsubstituted 2-aminothophene-3-carboxamide **6** and 2-aminocycloalkylthophene-3-carboxamide **8a-c**, we carried out Gewald reactions[26] using commercially available 2-cyanoacetamide **5**. The stable dimer of α-mercapto acetaldehyde, 1,4-dithiane-2,5-diol was condensed with **5** in the presence of triethylamine to afford **6** in 75% yield. Compound **8a-c** were also readily obtained by the condensation of the corresponding ketones with **5** in the presence of elemental sulfur and morpholine base in 65-73% yield. The Gewald condensation products **6** and **8a-c** were directly utilized for the next step without further purification. The amine **6** and **8a-c** were coupled with a variety of acyl chlorides to produce the corresponding amides **7a-c** and **9a-i** in 80-95% yield. The coupling of **8a-c** with various acyl chlorides and ammonium thiocyanate afforded the desired *N*-acylated thiourea derivatives[27] **10a-q** (65-88%).

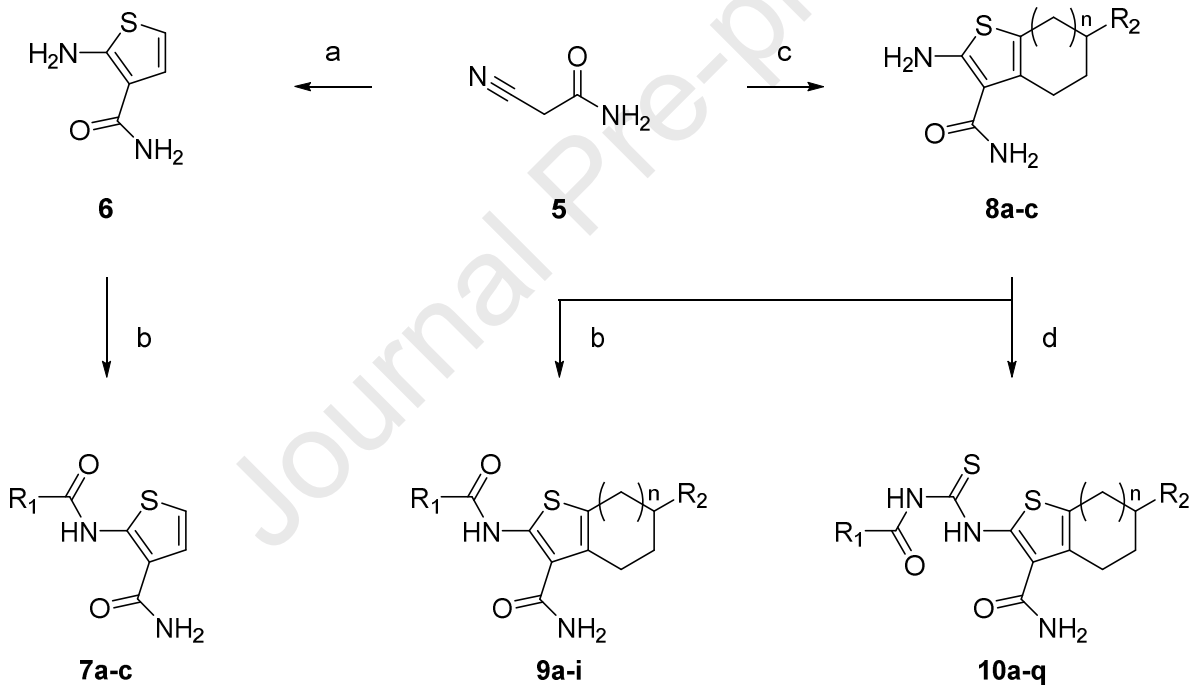

Scheme 1. Synthesis of 2-aminothiophene-3-carboxamide derivatives[a]

[a]Reagent and condition: (a) 1,4-dithiane-2,5-diol, Et_3N, EtOH, 70 °C, 6 h, 75%; (b) various acyl chlorides, pyridine, rt, 1 h, 80-95%; (c) various ketones, sulfur, morpholine, EtOH, 70 °C, 12 h, 65-73%; (d) various acyl chlorides, ammonium thiocyanate, acetone, reflux, 2 h, 65-88%.

2.2. Structure-Activity Relationships

Among several methods[28] for measuring ion channel modulation including electrophysiology patch-clamp assay, competitive binding assay with radiolabeled ligand, ion flux assay using radioactive tracers or fluorescence sensors, measurement of ionic current using patch-clamp has been considered to be most reliable indicator but it suffers from low-throughput. Fluorescent cellular membrane potential assay (FLIPR format) using fluorescence sensors offers high throughput efficiency and reproducible data. We have therefore adopted fluorescent cellular membrane potential assay[29] as a primary assay, followed by ion current assessment using patch clamp for secondary validation assay. We observed fluorescent cellular membrane potential assay data for the three references (**1**, **2**, and **3**) are in good agreement with patch clamp assay data, which is also accordance with reported IC_{50} values of **1** (2.1 μM)[30], **2** (1.1-1.8 μM)[23, 30], and **3** (77 nM)[23]. In the performance of the fluorescent cellular membrane potential assay, percent inhibitions at a single concentration (10 μM) were measured for all the derivatives, followed by estimation of IC_{50} values for the selected active (over 60% inhibiton) derivatives.

Table 1. Inhibitory-activities of **6**, **7a-c**, **8a-c** and **9a-i** against ANO1

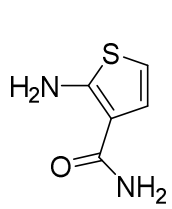

6

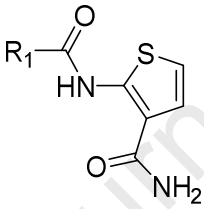

7a-c

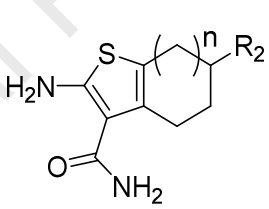

8a-c

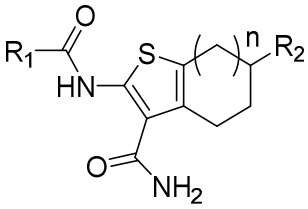

9a-i

Entry	R_1	n	R_2	% inhibition (%)[a]	IC_{50} (μM)	
				FLIPR format	FLIPR format	Patch clamp
1	-	-	-	92.88 ± 0.24	1.31 ± 0.77	1.53 ± 0.52
2	-	-	-	63.85 ± 0.28	2.60 ± 0.76	2.74 ± 0.78
3	-	-	-	73.77 ± 5.17	0.06 ± 0.02	0.03 ± 0.01
4				NA[c]	NA[c]	0.05 ± 0.01
6	-	-	-	inactive[b]		
7a	*tert*-butyl	-	-	inactive[b]		
7b	2-furyl	-	-	39.54 ± 5.24		
7c	phenyl	-	-	inactive[b]		
8a	-	0	H	15.44 ± 0.41		
8b	-	2	H	inactive[b]		
8c	-	1	*tert*-butyl	80.09 ± 0.75	2.95 ± 0.05	2.50 ± 0.19

9a	*tert*-butyl	0	H	12.51 ± 3.17		
9b	*tert*-butyl	2	H	67.94 ± 0.78	4.79 ± 1.10	4.07 ± 0.37
9c	*tert*-butyl	1	*tert*-butyl	86.87 ± 2.01	3.10 ± 1.23	2.56 ± 0.05
9d	2-furyl	0	H	51.49 ± 1.55		
9e	2-furyl	2	H	inactive[b]		
9f	2-furyl	1	*tert*-butyl	inactive[b]		
9g	phenyl	0	H	inactive[b]		
9h	phenyl	2	H	12.13 ± 9.65		
9i	phenyl	1	*tert*-butyl	21.99 ± 0.12		

[a] Average % inhibition value at 10 μM with S.D. are shown (mean ± S.D., n = 2)
[b] Maximum inhibition is less than 10% at 10 μM
[c] Not applicable

As shown in Table 1, among four C-4 and C-5 unsubstituted 2-aminothophene-3-carboxamides tested, three derivatives (**6**, **7a**, and **7c**) are inactive and **7b** having 2-furyl amide functional group exhibits a moderate ANO1 inhibitory activity (39.54% inhibition at 10 μM) in fluorescent cellular membrane potential assay. Fusion of 2-aminothophene-3-carboxamide (**6**) with unsubstituted cyclopentane (**8a**) or cycloheptane (**8b**) has little or no influence on activity as **8a** exhibits little activity and **8b** is inactive like **6**. In contrast, *tert*-butyl group substituted cyclohexane-fused 2-aminothophene-3-carboxamide (**8c**) displays excellent activity with IC_{50} value of 2.95 μM in fluorescent cellular membrane potential assay, which is confirmed in electrophysiology patch clamp assay (IC_{50} = 2.50 μM). It is worth noting that this fusion with *tert*-butylcyclohexane was inspired by **1** and ANO1 inhibitory activities of **8c** are comparable to those (IC_{50} = 1.31 μM from fluorescent cellular membrane potential assay, 1.53 μM from patch clamp assay) of **1**. We next introduced a variety of acyl groups on 2-aminocycloalkylthiophene-3-carboxamides to generate **9a-i** and investigated the effects of the acylations. In contrast to the observation that installation of *tert*-butyl amide on **8a** having cyclopentane ring has no influence on activity (**9a**), the incorporation of *tert*-butyl amide on inactive **8b** possessing cycloheptane ring was found to lead dramatically to a highly active derivative (**9b**) with IC_{50} values of around 4 μM from both fluorescent cellular membrane potential and patch clamp assays. Meanwhile, no differences in potency were observed between very potent **8c** bearing *tert*-butylcyclohexane group and **9c** obtained by introduction of *tert*-butyl amide on **8c**. It is worthwhile to note that **9c** exhibits the highest percentage (86.87%) of inhibition at single concentration (10 μM) in fluorescent cellular membrane potential assay among all our derivatives tested and displays great IC_{50} values of 3.10 μM and 2.56 μM in fluorescent cellular membrane potential and patch clamp assays, respectively. We next adopted 2-furyl amide group incorporated in **1** and explored the effects of 2-furyl amide functionality. In contrast to the contribution of *tert*-butyl

amide group to ANO1 inhibitory activity exemplified by **9b**, introduction of 2-furyl amide group on **8b** has no influence on activity (**9e**) even though the activity of **9d** installed with 2-furyl amide is increased by around two-folds compared with **8a**. To our surprise, incorporation of 2-furyl amide on potent **8c** causes complete abolition of activity (**9f**).

Our attention next turned to an evaluation of the effects of acylthiourea functionality on 2-aminocycloalkylthiophene-3-carboxamide in comparison with amide functionality. Acylthiourea group has been adopted for a variety of medicinal chemistry researches including PBD inhibitors[31], 15-lipoxygenase inhibitors[27], and histone deacetylase-8 activators[32]. Benzoylthiourea is absolutely superior to benzamide functionality in terms of the degree of contribution to ANO1 inhibitory activities of 2-aminocycloalkylthiophene-3-carboxamides. To our surprise, inactive **9g** and almost inactive **9i** were converted into a potent derivative **10a** (IC_{50} = 2.83 μM from fluorescent cellular membrane potential assay, 2.63 μM from patch clamp assay) and an active derivative **10c** by substitution of benzamide group with benzoylthiourea group. The contribution of benzoylthiourea group to ANO1 inhibitory activity was not observed on 2-aminothiophene-3-carboxamide fused with cycloheptane ring (**10b**) in comparison between activities of **9h** (12.13% inhibition at 10 μM) and **10b** (21.13% inhibition at 10 μM). Encouraged by the contribution of benzoylthiourea group to activity exemplified with **10a** and **10c**, we next investigated the effects of 2-furoylthiourea and thiazole-5-carbonylthiourea. In contrast to benzoylthiourea group, substitutions of furan-2-amide group on **9d** and **9e** with 2-furoylthiourea group result in decreased activity (**10d**) and almost unaltered activity (**10e**). Likewise, thiazole-5-carbonylthiourea functionality on **10g** is not capable of enhancing activity. Our attention next focused on investigating effects of substituents on the benzoylthiourea group in order to improve potency of **10a**. Unfortunately, neither electron-donating substituents (**10g-l**) nor electro-withdrawing substituents (**10m-q**) increase ANO1 inhibitory in comparison to the potency of **10a** having unsubstituted benzoylthiourea functionality. The electron-donating substituents (**10g-l**) and trifluoromethyl substituent (**10m-n**) cause little to no activities but 2-chloro (**10o**) and 4-chloro (**10q**) substituents result in maintained activities compared with the activities of **10a**. Interestingly, 3-chloro substituent (**10p**) causes abolished activity. It is worth recalling that replacement of benzamide group on inactive **9g** with benzoylthiourea group dramatically causes high potency indicating that benzoylthiourea functionality substantially contributes to ANO1 inhibitory activity. The activity (IC_{50} = 1.75 μM from patch clamp assay) of **10q** bearing 4-chloro substituted benzoylthiourea group in patch clamp assay is only marginally higher than that (IC_{50} = 2.63 μM from patch clamp assay) of **10a**.

Table 2. Inhibitory-activities of **10a-q** against ANO1

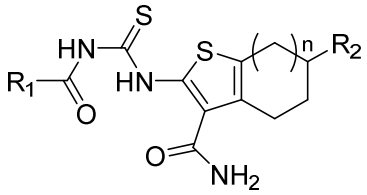

10a-q

Entry	R_1	n	R_2	% inhibition (%)[a]	IC_{50} (μM)	
				FLIPR format	FLIPR format	Patch clamp
10a	phenyl	0	H	70.50 ± 0.00	2.83 ± 0.96	2.63 ± 0.47
10b	phenyl	2	H	21.13 ± 16.94		
10c	phenyl	1	*tert*-butyl	70.28 ± 8.76	3.09 ± 1.07	5.66 ± 0.57
10d	2-furyl	0	H	inactive[b]		
10e	2-furyl	2	H	21.75 ± 4.32		
10f	2-furyl	1	*tert*-butyl	13.79 ± 3.75		
10g	4-methylthiazol-5-yl	0	H	inactive[b]		
10h	3,4-dimethoxyphenyl	0	H	inactive[b]		
10i	3,5-dimethoxyphenyl	0	H	46.07 ± 0.92		
10j	3,4,5-trimethoxyphenyl	0	H	inactive[b]		
10k	1,3-benzodioxol-5-yl	0	H	16.33 ± 14.22		
10l	2,3-dihydro-1,4-benzodioxin-6-yl	0	H	12.28 ± 3.85		
10m	3-(trifluoromethyl)phenyl	0	H	26.69 ± 7.61		
10n	4-(trifluoromethyl)phenyl	0	H	inactive[b]		
10o	2-chlorophenyl	0	H	76.70 ± 10.75	2.29 ± 0.30	3.12 ± 0.27
10p	3-chlorophenyl	0	H	inactive[b]		
10q	4-chlorophenyl	0	H	72.25 ± 11.78	2.36 ± 0.79	1.75 ± 0.30

[a] Average % inhibition value at 10 μM with S.D. are shown (mean ± S.D., n = 2)
[b] Maximum inhibition is less than 10% at 10 μM

2.3. Endogenous ANO1 expression level in both normal cells and GBM cells

It has been reported that ANO1 is highly expressed in GBM cell lines such as U87MG[12], U138[13] and U251[14]. Glioma is divided into I-IV according to the pathological grade. The degree of mRNA and protein expression of ANO1 is increased with increasing disease grade[12]. It has been

reported that inhibition of ANO1 expression by siRNA inhibits cell proliferation[12], invasion and migration[14] in GBM cell line U87MG. In order to select GBM cell lines with high expression level of ANO1, we measured the mRNA level and protein expression level of ANO1 using qRT-PCR and western blot analysis.

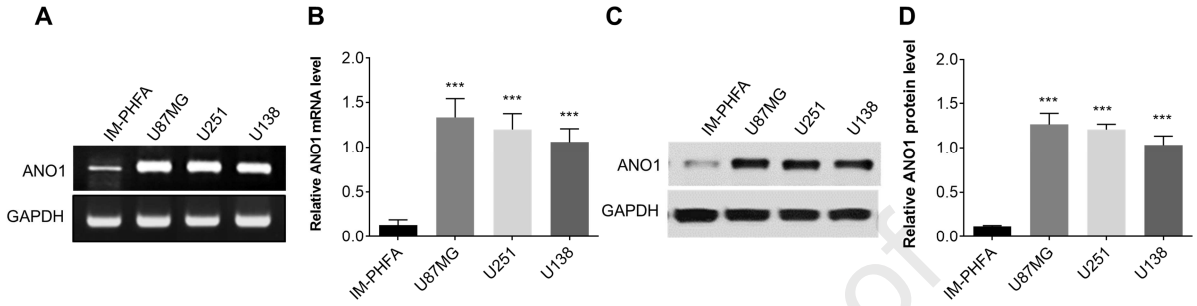

Figure 2. Expression level of endogenous ANO1 in various GBM cell lines and normal cells. (A) Expression level of endogenous ANO1 mRNA. (B) Quantification for expression level of endogenous ANO1 mRNA using ImageJ. (C) Expression level of endogenous ANO1 protein. (D) Quantification for expression level of endogenous ANO1 protein using ImageJ. (B, D) statistics analysis was evaluated by using Prism version 6.0. Band densities were measured using ImageJ software and shown in the bar graph (mean ± SD, two-tailed Student's t-test, **** $p < 0.0001$, *** $p < 0.001$, ** $p < 0.01$, ns: not significant).

We also compared the levels of mRNA and protein of ANO1 between normal IM-PHFA (human fetal astrocyte) cells and three GBM cell lines (U87MG, U251 and U138) (Fig. 2). The expression level of ANO1 mRNA turned out to be very low in normal brain cells, IM-PHFA (0.13 ± 0.06). The mRNA expression level of ANO1 in U251 (1.20 ± 0.17) and U87MG (1.30 ± 0.21) divided into Grade IV is slightly higher than that (1.06 ± 0.15) in U138 (Fig. 2A-B). As expected, the expression level of ANO1 protein in IM-PHFA cells is very low (0.12 ± 0.01) and the level of ANO1 protein expression in both U251 (1.21 ± 0.06) and U87MG (1.27 ± 0.12) is higher than that (1.03 ± 0.10) in U138 (Fig. 2C-D).

2.4. 2D and 3D Anti-proliferative effects of 9c and 10q in GBM cell lines

Inhibition of ANO1 by siRNA suppresses cancer cell viability in GBM[12], breast cancer[3], prostate carcinoma[5] and ovarian cancer[33]. In addition, ANO1 channel blocker **1** significantly suppresses the growth of breast cancer cells[3]. Based on the ANO1 inhibitory activities estimated in both fluorescent cellular membrane potential and patch clamp assays, we selected seven potent derivatives and assessed their anti-proliferative activities on three GBM cell lines having high expression level of ANO1 mRNA and protein.

Table 3. Anti-proliferative effects of selected derivatives

Entry	GI_{50} (μM)[a]			
	Mouse primary astrocyte	U251	U87MG	U138
1	inactive[b]	41.89 ± 3.38	inactive[b]	89.38 ± 7.06
2	inactive[b]	79.27 ± 8.09	inactive[b]	inactive[b]
3	inactive[b]	36.48 ± 0.54	32.98 ± 2.16	32.44 ± 2.23
4	inactive[b]	45.33 ± 0.59	48.00 ± 5.18	29.40 ± 1.22
8c	inactive[b]	83.24 ± 5.07	inactive[b]	inactive[b]
9b	inactive[b]	inactive[b]	inactive[b]	inactive[b]
9c	94.83 ± 4.13	12.58 ± 0.75	31.49 ± 0.60	22.24 ± 0.65
10a	inactive[b]	24.37 ± 1.61	25.96 ± 2.23	17.05 ± 0.59
10c	inactive[b]	70.18 ± 0.74	82.35 ± 3.29	inactive[b]
10o	inactive[b]	94.60 ± 3.11	inactive[b]	inactive[b]
10q	45.15 ± 0.85	12.04 ± 0.20	23.77 ± 10.39	13.22 ± 0.72

[a] Cell Titer-glo assay results. Average GI_{50} values with S.D. (n = 3, duplicate) are shown.
[b] Maximum inhibition <50% at 100 μM.

Among the selected seven derivatives, anti-proliferative activities of **9c, 10a** and **10q** in three GBM cell lines (U251, U87MG and U138) turned out to be higher than those of the three reference compounds (**1, 2** and **3**). As shown in Table 3, the GI_{50} values of **9c, 10a** and **10q** in U251 glioma cells are 12.58 μM, 24.37 μM and 12.04 μM, respectively, which are superior to those (41.89 μM, 79.27 μM, 36.48 μM and 45.33 μM, respectively) of four references **1**, **2**, **3** and **4**. We also examined whether our ANO1 inhibitors possess differential cytotoxic effects between glioma cancer cells and normal brain cells, primary astrocytes derived from adult mouse brain. It was found that **9c, 10a** and **10q** have little to no effects on primary astrocytes and are capable of discriminating between glioma cells and normal brain cells (Table 3). It is worthwhile recalling that ANO1 inhibitory activities of **9c, 10a** and **10q** are inferior to those of **3** and **4** and comparable to those of both **1** and **2**. It is not likely that ANO1 inhibitory activities of all compounds tested in this study are well translated into anti-proliferative effects in GBM cells. Reference compound **3** and **4** possess potent ANO1 inhibitory activities but display moderate GI_{50} values of 36.48 μM and 45.33 μM, respectively on U251 cells. Also, anti-proliferative activities of both **1** and **2** on U251 glioma cells appear to be low in comparison to their ANO1 inhibitory potencies with IC_{50} values of around 2 μM. Meanwhile, it is worth noting that **3** has low plasma stability[24], which might contribute to its moderate anti-proliferative activity in GBM cells.

Based on the growth inhibitory activities (GI_{50}s), endogenous ANO1 expression level and glioma cell morphology, we selected U251 among three GBM cell lines to perform further

experiments. In addition, both **9c** and **10q** were elected as representative compounds as they significantly suppress the proliferation of U251 glioma cells with GI_{50} values of less than 20 μM (Table 3).

Anchorage independent growth (AIG) is one of the hallmarks of tumorigenesis and AIG assay has been considered as the most reliable *in vitro* method to detect cell transformation. The theoretical basis for this technique relies on extracellular matrix (ECM) contact for normal cell growth and division, but cancer cells have capability to grow and differentiate without affecting the surrounding environment. Inhibition of ANO1 by siRNA results in a reduction of soft agar colony formation on ovarian cancer[33] and colorectal cancer[34] cells. To investigate if both **9c** and **10q** are capable of blocking tumorigenesis of ANO1-expressed GBM cells, we carried out colony formation assay (2D) and soft agar assay (3D) in U251 glioma cells. Incubation with each compound at three different concentrations (1, 3 and 10 μM) for 14 days suppressed anchorage-independent growth in terms of colony number of U251 cells.

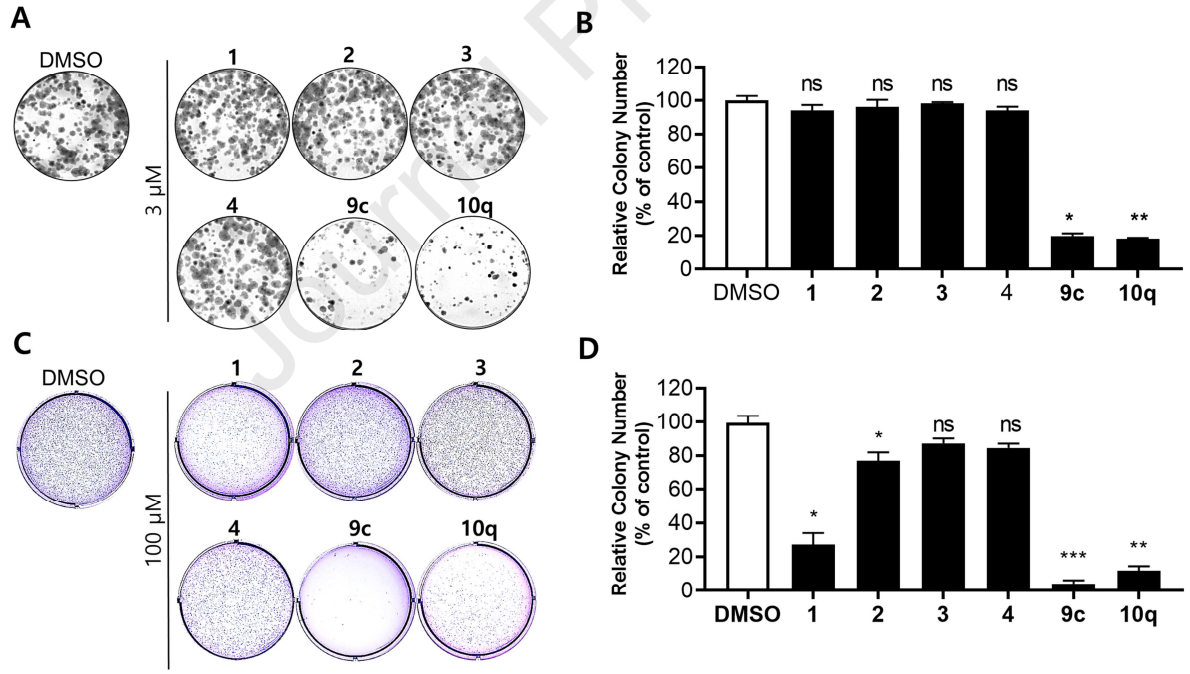

Figure 3. Inhibition of ANO1 suppresses tumor cell growth in U251 GBM cells. (A) Colony formation assay (2D) in U251 GBM cells. (C) Anchorage independent growth (3D) of U251 GBM cells. Cells embedded in 0.3% top agar were incubated with indicated concentrations of compounds for 14 days and colonies were observed (n = 3) (B, D) The results were compared to DMSO control. Average number of colonies per well was automatically counted using ImageJ software and shown in

the bar graph (mean ± SD, two-tailed Student's t-test, **** $p < 0.0001$, *** $p < 0.001$, ** $p < 0.01$, ns: not significant).

In contrast to both **9c** and **10q**, none of three reference compounds (**2**, **3** and **4**) exhibited effects at even 10 μM in two-dimensional colony formation analysis. However, 10 μM of **1** showed an inhibitory effect. The degree (72.71%) of inhibition by **1 (**10 μM) is similar to that promoted by 3 μM of **9c** or **10q**. Compound **9c** and **10q** at 10 μM concentration showed an inhibitory effect of 96.58% and 96.40%, respectively, which indicates that both **9c** and **10q** possess a concentration-dependent inhibitory effect (Fig. 3A-B, Fig. S1). In the soft agar analysis (3D), colony formation was not suppressed at 10 μM concentration of all compounds tested and three-dimensional soft agar assays were carried out with increased concentration (30 and 100 μM) of test compounds. None of three reference compounds (**2**, **3** and **4**) displayed an inhibitory effect even at 100 μM but **1** showed an inhibitory effect (72.65%) at 100 μM even though 30 μM of **1** exhibited no effect. Derivative **9c** and **10q** at 100 μM concentration strongly suppressed colony formation by 95.70% and 88.05%, respectively and showed dose-dependency in three-dimensional soft agar assay (Fig. 3C-D, Fig. S1). Taken together, both **9c** and **10q** turned to be superior to the three reference compounds (**1**, **2** and **3**) in terms of capability of inhibiting colony formation in both 2D colony formation assay and 3D soft agar assay using U251 glioma cells.

2.5. Inhibitory effects of 9c and 10q on migration and invasion of U251 GBM cells

Inhibition of ANO1 by shRNA or siRNA blocks cellular migration and invasion in GBM, anaplastic thyroid cancer[35] and ovarian cancer[33]. In addition, ANO1 channel inhibitor **2** suppresses migration and invasion of U251 GBM cells[13]. In order to identify derivatives possessing remarkable migration-inhibitory activity, a typical scratch wound healing assay was conducted with 5 μM (Fig. S2) of selected seven derivatives of which IC_{50} values are less than 3 μM in the Cell Titer-Glo assay. Among these seven derivatives, both **9c** and **10q** significantly suppressed migration of U251 cells. We next assessed dose-dependent effects of **9c** and **10q** and observed that both **9c** and **10q** significantly blocked migration of U251 cells in a dose-dependent manner (Fig. 4A-B). In addition, both **9c** and **10q** also strongly suppressed invasion of U251 cells at 10 μM in Boyden chamber invasion assay (Fig. 4C-D). Indeed, migration and invasiveness of U251 cells were decreased up to 90% by **9c** (10 μM). It was observed that **1, 2**, **3** and **4** at 10 μM concentration reduced migration of U251 cells by 34.83%, 26.53%, 10.45% and 16.74%, respectively (Fig. 4A-B) and decreased invasion of U251 cells by 28.33%, 19.17%, 12.10% and 11.73%, respectively (Fig. 4C-D), which indicates that both **9c** and **10q** are superior to **1, 2**, **3** and **4** in terms of capability of suppressing both migration and invasion of U251 cells. Based on the report that knockdown of ANO1 using siRNA is related to

increase the expression E-cadherin in breast cancer cells[36], we investigated if the level of E-cadherin in U251 glioma cells is increased by the treatment of **9c** and **10q** and observed that both substances cause increase of E-cadherin in concentration-dependent fashion (Fig. 4E-F). We also investigated the effects of both **9c** and **10q** on ANO1 protein level in U251 glioma cells. The western blot analysis reveals that both **9c** and **10q** cause ANO1 protein degradation in U251 cells and this ANO1 degradation is blocked by the treatment of MG132, a proteasome inhibitor (Fig. 4G).

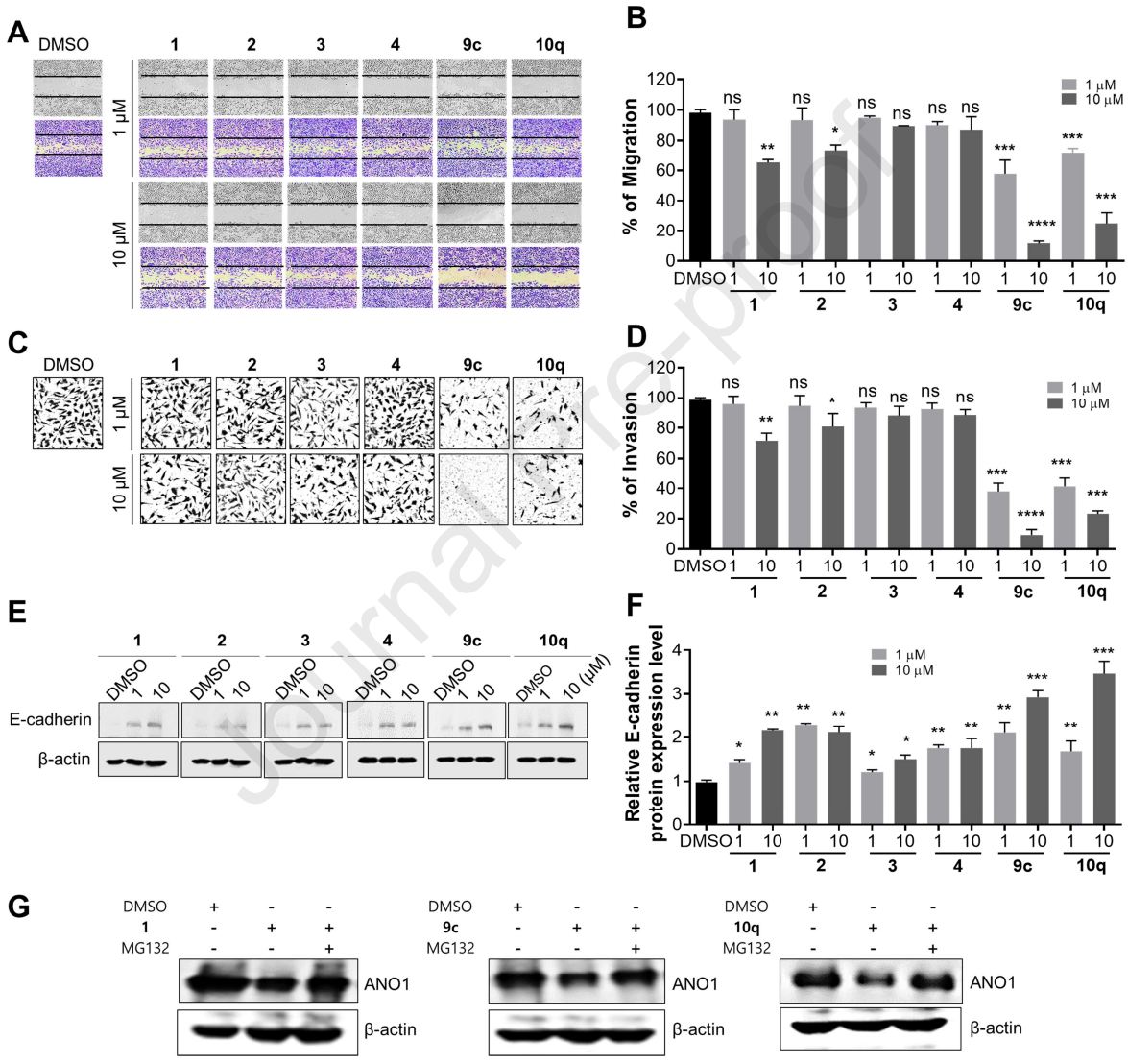

Figure 4. Derivative **9c** and **10q** suppress migration and invasion of U251 GBM cells. (A) Each compound treated at 10 μM concentration, were incubated for 18 h after scratching cell monolayer. Migration ratio was calculated using migration area using ImageJ. (C) Invasion assays were performed using CHEMICON QCM 24 well invasion assay kit. Invasion assay ratio were calculated using colorimetric reading of OD at 560 nm. (E) Representative western marker related ANO1. Analysis of EMT (Epithelial–mesenchymal transition) marker, E-cadherin. Quantification of western

band was analysis using band density using ImageJ. (G) U251 cells were incubated with 10 μM concentration of the inhibitors (**1, 9c** or **10q**) for 24 h. Also, U251 cells were incubated with 10 μM concentration of the inhibitors (**1, 9c** or **10q**) for 6 h, followed by the treatment of MG132 (20 μM) for an additional 18 h. (B, D, F) Significant differences were calculated using a one-way ANOVA (* $p < 0.05$; ** $p < 0.01$; *** $p < 0.001$; **** $p < 0.0001$).

2.6. Electrophysiologic effects of 9c and 10q

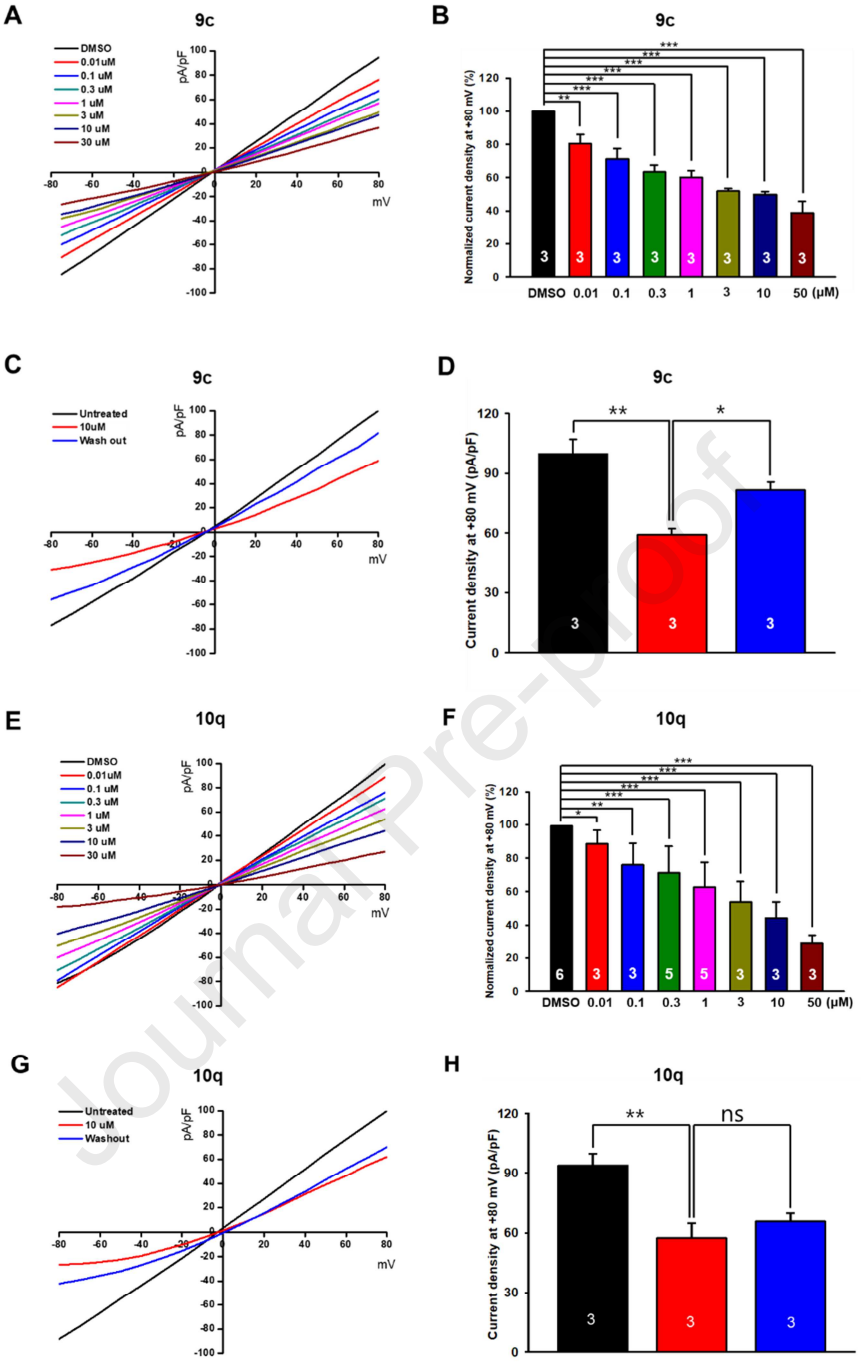

Figure 5. Both **9c** and **10q** suppress ANO1 channel activities in HEK293 cells transfected with ANO1. (A, E) inhibitory effects of **9c** and **10q** on ANO1 current amplitude at +80 mV. Error bars represent SD. (B, F) normalized current density at +80 mV. The n values for each statistical analysis are indicated at histograms. (C, G) inhibitory effects of **9c** (10 μM) and **10q** (10 μM) on ANO1 current amplitude at +80 mV. Error bars represent SD. (D, H) normalized current density at +80 mV. The n value for each statistical analysis is 3. Significant differences were calculated using a one-way ANOVA. (* p <0.05; ** p <0.01; *** p< 0.001; **** p< 0.0001).

In order to evaluate the effects of **9c** and **10q** on ANO1 channel currents, whole-cell recordings were carried using HEK293A cells transfected with GFP-mANO1 channel plasmids (Fig. 5). As depicted in Figure 5B and 5F, both **9c** and **10q** effectively inhibit ANO1-mediated currents in dose-dependent manner. ANO1 currents were inhibited by 50.64% and 57.63% at 10 μM concentration of **9c** and **10q**. IC_{50} values of **9c** and **10q** were estimated to be 2.56 μM and 1.75 μM respectively for inhibition of ANO1-mediated currents. These results clearly indicate that both **9c** and **10q** are capable of inhibiting channel activity of ANO1. In addition, to examine the reversibility of ANO1 inhibition caused by **9c** and **10q**, we measured the ANO1-mediated currents after washout of compound **9c** and **10q**. Reduced ANO1-mediated currents by **9c** were partially recovered after washout. The amplitude of ANO1-mediated currents was recovered up to 85.80% compared to the currents prior to the treatment of **9c** (Fig. 5C-D), which reveals that **9c** possesses reversible inhibitory effect on ANO1-mediated currents. However, reduced ANO1-mediated currents by **10q** were not recovered after washout, indicating that **10q** irreversibly inhibits ANO1 channel activity. In addition to **9c** and **10q**, other derivatives **8c, 9b, 10a, 10c** and **10o** were also submitted to whole-cell patch clamp assay using GFP-mANO1 transfected HEK293A cells and their effects on ANO1 channel currents are described in Figure S3.

On the basis of a previous report that ANO1 is highly expressed in U251 glioma cells[13]. We next examined the effects of **9c** and **10q** on ANO1 currents in U251 cells and observed that ANO1-mediated currents are inhibited about 40 % and 60% respectively by 10 μM of **9c** and **10q**, ANO1 channel blockers (Fig. S4), which demonstrates that **9c** and **10q** have capability of inhibiting ANO1 currents in a glioma cells as well as in HEK293A cells transfected with ANO1.

Our attention next turned into the evaluation of selectivity of both **9c** and **10q** in inhibiting ion channel activities. In order to make comparison between inhibitory effects of **9c** and **10q** on ANO1, ANO2 and TTYH-1 channels which belongs to a family of human high-conductance chloride ion channels, we obtained current-voltage (*I-V*) curves using HEK293A cells transfected with GFP-mANO1, GFP-mANO2 or GFP-mTTYH-1. As shown in Figure 6A and B, apical membrane current measurement in HEK293A cells expressing GFP-mANO1, GFP-mANO2 or GFP-mTTYH-1 revealed that ANO1 is more strongly inhibited rather than ANO2 and TTYH-1 is not inhibited by both **9c** and **10q**. Both **9c** and **10q** strongly inhibit ATP-induced ANO1 chloride currents in a dose dependent manner with IC_{50} values of 2.56 μM and 1.75 μM but slightly suppress ANO2 with IC_{50} values of 15.43 μM and 7.43 μM. It is worth recalling that ANO2 knockout mice exhibits severe cerebellar motor learning deficits[17] and selective ANO1 blockers over ANO2 are obviously favarable to avoid potential toxicities. It is challenging to obtain selectivity for ANO1 inhibition over ANO2 inhibition as

ANO1 and ANO2 are highly homologous. It should be noted that both **9c** and **10q** are selective ANO1 blockers over ANO2 and TTYH-1 chloride ion channel.

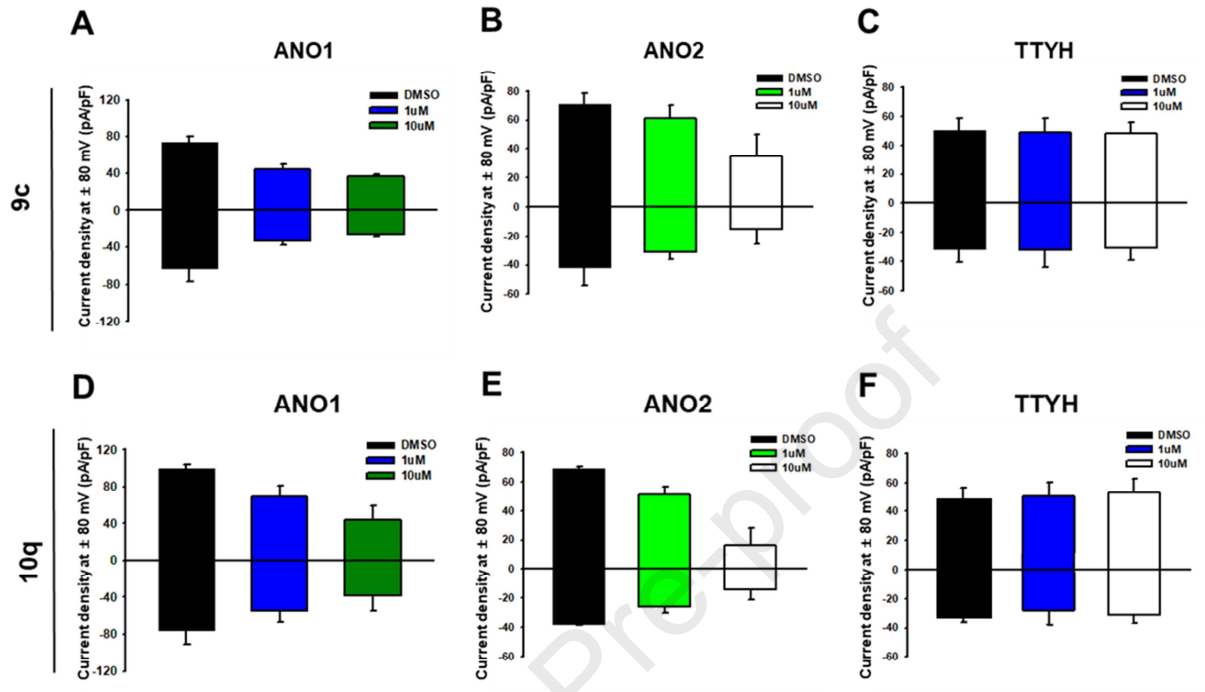

G

Entry	IC_{50} (μM)		
	ANO1	ANO2	TTYH-1
9c	2.56	15.43	inactive [a]
10q	1.75	7.43	inactive [a]

Figure 6. Selective inhibition of ANO1 over ANO2 and TTYH-1 by **9c** and **10q**. (A, D) inhibition of ANO1 channel activity by **9c** and **10q**. (B, E) inhibition of ANO2 channel activity by **9c** and **10q** (C, F) inhibition of TTYH-1 channel activity by **9c** and **10q**. The n value for each statistical analysis is 3. (G) IC_{50} values of **9c** and **10q**.

2.7. Combination treatment of 9c with temozolomide (TMZ) in U251 cells

As aforementioned, effective therapeutics against recurrent GBM are still very limited even though surgical resection followed by radiotherapy and chemotherapy with temozolomide (TMZ)[37] has become the first-line therapy against GBM. It was reported that the level of mRNA and protein expression of ANO1 increases with increasing disease grade in GBM patients[12]. We hypothesized that the combination of ANO1 inhibitors and TMZ would result in synergistic effects in suppressing proliferation of glioma cells and for the first time, to the best of our knowledge, examined synergistic effect of combination of an ANO1 inhibitor (**9c** or **3)** and TMZ in U251 glioma cells.

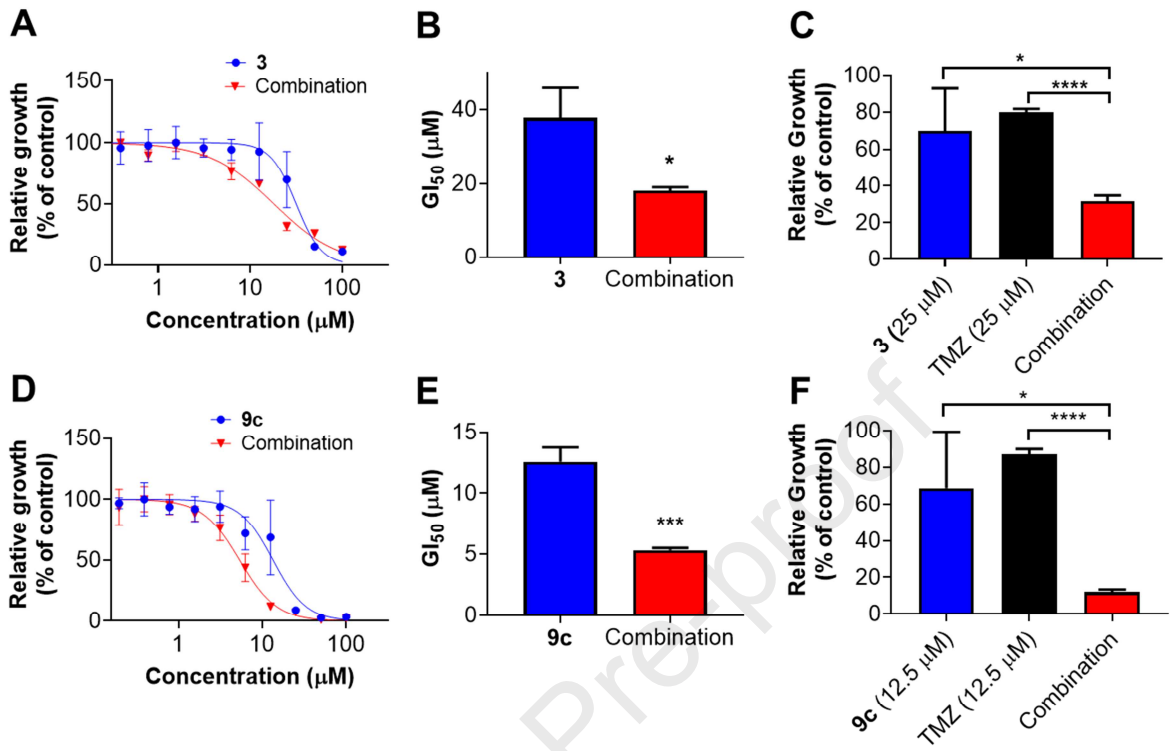

G

	GI_{50} (μM) [a]		CI value	Description
	Single	Combination		
3	37.71 ± 8.12	18.06 ± 0.97	0.701 ± 0.03	Moderate synergism
9c	12.58 ± 0.75	5.32 ± 0.20	0.647 ± 0.03	Synergism

[a] Cell Titer-glo assay results. Average GI_{50} values with S.D. (n = 3, duplicate) are shown.

Figure 7. Synergistic effects of combination of ANO1 inhibitor (**9c** or **3**) and TMZ in suppressing proliferation of U251 cells. (A, D) full titration curve for **3** or **9c** combined with TMZ (B, E) histogram for GI_{50} values (C, F) effects of **3** or **9c** combined with TMZ on the proliferation of U251 cells. (G) GI_{50} and CI values of **3** and **9c** combined with TMZ. Significant differences were calculated using a one-way ANOVA (* $p < 0.05$; ** $p < 0.01$; *** $p < 0.001$; **** $p < 0.0001$).

As depicted in figure 7, appreciable synergistic effects of combination of ANO1 inhibitor and TMZ were observed and effect of **9c** combined with TMZ is superior to that of **3** combined with TMZ. GI_{50} value (5.32 μM) of **9c** combined with TMZ is decreased by more than 50% compared with that (GI_{50} = 12.58 μM) of **9c** alone. CI value of **9c** combined TMZ (TMZ : **9c** = 1:1) is 0.63 ± 0.03 ($0.4 < CI < 0.7$, synergism). GI_{50} value of **3** combined with TMZ is decreased by more than 40% with

CI value of 0.70 ± 0.03 (0.7< CI < 0.85, moderate synergism). CI values were estimated using compusyn software.

3. Conclusions

Glioblastoma (GBM) is one of the most aggressive cancers with poor prognosis with median survival for 15 months. Lack of effective treatment options against GBM emphasizes urgent necessity of effective GBM therapeutics. ANO1, a calcium-activated chloride ion channel (CaCC), is over-expressed in GBM and inhibition of ANO1 has been reported to suppress cell proliferation, migration and invasion in GBM. In order to identify potent and selective ANO1 inhibitors capable of inhibiting GBM cells, we have designed and synthesized a series of new 2-aminothiophene-3-carboxamide derivatives. We performed SAR study using fluorescent cellular membrane potential membrane potential assay as a primary assay, followed by ion current assessment using patch clamp for secondary validation assay and selected seven derivatives that effectively inhibit ANO1 channel activity with IC_{50} values ranging from 1.75 μM to 5.66 μM. It should be noted that manual whole-cell patch clamp, the gold standard of electrophysiological method, requires a high expertise and a lot of efforts with a very low throughput. These seven substances were submitted to anti-proliferation assay using GBM cells and two lead compounds (**9c** and **10q)** were identified. Unique structural feature of **10q**, a cyclopentane-fused thiophene-3-carboxamide derivative, is the presence of benzoylthiourea functionality which dramatically contributes to activity. Both **9c** and **10q** suppress more strongly proliferation of GBM cells than four reference compounds including **3**, Ani-9. ANO1 blocker **9c** and **10q** are also capable of inhibiting much more strongly colony formation than reference compounds in both 2D colony formation assay and 3D soft agar assay using U251 glioma cells. In addition, **9c** and **10q** suppress far more strongly migration/invasion of GBM cells than reference compounds. Whole-cell patch clamp recordings were carried out to confirm activities of seven inhibitors selected from fluorescent cellular membrane potential assay. ANO2 knockout mice was reported to exhibit severe cerebellar motor learning deficits and selective ANO1 blockers over ANO2 are obviously favarable to avoid potential toxicities. Satisfyingly, both **9c** and **10q** turned to be selective ANO1 blockers over ANO2 and TTYH-1 chloride ion channel. It is challenging to obtain selectivity for ANO1 inhibition over ANO2 inhibition as ANO1 and ANO2 are highly homologous. We, for the first time, found that the combination of ANO1 inhibitor (**9c** or **3**) and TMZ brings about remarkable synergistic effects in suppressing proliferation of GBM cells. Our study may provide an insight into designing selective and potent ANO1 inhibitors as pharmacological tools as well as promising leads for novel GBM drug discovery.

4. Experimental Section

4.1 Chemistry

Unless otherwise described, all commercial reagents and solvents were purchased from commercial suppliers and used without further purification. All reactions were performed under N_2 atmosphere in flame-dried glassware. Reactions were monitored by TLC with 0.25 mm E. Merck precoated silica gel plates (60 F254). Reaction progress was monitored by TLC analysis using a UV lamp, ninhydrin, or *p*-anisaldehyde stain for detection purpose. All solvents were purified by standard techniques. Purification of reaction products was carried out by silica gel column chromatography using Kieselgel 60 Art. 9385 (230–400 mesh). The purity and of all compounds was over 95% and mass spectra and purity of all compounds was analyzed using Waters LCMS system (Waters 2998 Photodiode Array Detector, Waters 3100 Mass Detector, Waters SFO System Fluidics Organizer, Water 2545 Binary Gradient Module, Waters Reagent Manager, Waters 2767 Sample Manager) using SunFireTM C18 column (4.6 × 50 mm, 5 μm particle size): solvent gradient = 90% A at 0 min, 0% A at 5 min. Solvent A = 0.1% TFA in H_2O; Solvent B = 0.1% TFA in MeCN; flow rate : 2.0 mL/min. ^1H and ^{13}C NMR spectra were obtained using a Bruker 400 MHz FT-NMR (400 MHz for ^1H, and 100 MHz for ^{13}C) spectrometer. Standard abbreviations are used for denoting the signal multiplicities.

2-Aminothiophene-3-carboxamide (6) To a suspension of 1,4-dithiane-2,5-diol (9.1 g, 59.8 mmol) and 2-cyanoacetamide (5.0 g, 59.8 mmol) in EtOH (60.0 mL) was added triethylamine (16.3 mL, 119.6 mmol) at room temperature. The reaction mixture was stirred at 70 ^oC for 6 h. The reaction mixture was cooled to room temperature, diluted with EtOAc and quenched with H_2O. The organic layer was washed with brine, dried over $MgSO_4$, filtered and concentrated. The residue was dissolved in CH_2Cl_2 and solidified by adding Et_2O. The resulting solid was collected to afford **6** (6.4 g, 75%) as a brown solid. ^1H NMR (400 MHz, DMSO-d_6) δ 7.21 (s, 2H), 7.21 (brs, 1H), 7.04 (d, J = 5.7 Hz, 1H), 6.71 (brs, 1H), 6.22 (d, J = 5.7 Hz, 1H); ^{13}C NMR (100 MHz, DMSO-d_6) δ 167.68, 161.80, 124.94, 107.20, 105.56; LRMS (ESI) *m/z* 143 $[M + H]^+$.

2-Amino-5,6-dihydro-4*H*-cyclopenta[*b*]thiophene-3-carboxamide (8a) To a suspension of 2-cyanoacetamide (3.0 g, 35.7 mmol), cyclopentanone (3.2 mL, 35.7 mmol), and morpholine (7.1 mL, 71.4 mmol) in EtOH (60.0 mL) was added sulfur (1.1 g, 35.7 mmol) at room temperature. The reaction mixture was stirred at 70 ^oC for 12 h. The reaction mixture was cooled to room temperature, diluted with EtOAc and quenched with H_2O. The organic layer was washed with brine, dried over $MgSO_4$, filtered and concentrated. The residue was dissolved in CH_2Cl_2 and solidified by adding Et_2O. The resulting solid was collected to afford **8a** (3.7 g, 73%) as a brown solid. ^1H NMR (400 MHz,

DMSO-d_6) δ 7.15 (s, 2H), 6.43 (brs, 2H), 2.77 (t, J = 7.0 Hz, 2H), 2.63 (t, J = 7.2 Hz, 2H), 2.25 (m, 2H); ^{13}C NMR (100 MHz, DMSO-d_6) δ 167.69, 165.63, 139.94, 119.59, 103.02, 29.81, 28.27, 26.95; LRMS (ESI) *m/z* 227 $[M + H]^+$.

2-Amino-5,6,7,8-tetrahydro-4*H*-cyclohepta[*b*]thiophene-3-carboxamide (8b) To a suspension of 2-cyanoacetamide (3.0 g, 35.7 mmol), cycloheptanone (4.2 mL, 35.7 mmol), and morpholine (7.1 mL, 71.4 mmol) in EtOH (60.0 mL) was added sulfur (1.1 g, 35.7 mmol) at room temperature. The reaction mixture was stirred at 70 ^{o}C for 12 h. The reaction mixture was cooled to room temperature, diluted with EtOAc and quenched with H_2O. The organic layer was washed with brine, dried over $MgSO_4$, filtered and concentrated. The residue was dissolved in CH_2Cl_2 and solidified by adding Et_2O. The resulting solid was collected to afford **8b** (4.9 g, 65%) as a brown solid. ^{1}H NMR (400 MHz, DMSO-d_6) δ 6.81 (brs, 1H), 6.03 (s, 1H), 2.67 (m, 2H), 2.52 (m, 2H), 1.73 (m, 2H), 1.55 (m, 4H); ^{13}C NMR (100 MHz, DMSO-d_6) δ 167.81, 153.47, 136.20, 119.88, 113.29, 31.57, 28.43, 28.21, 27.71, 27.09; LRMS (ESI) *m/z* 237 $[M + H]^+$.

2-Amino-6-(*tert*-butyl)-4,5,6,7-tetrahydrobenzo[*b*]thiophene-3-carboxamide (8c) To a suspension of 2-cyanoacetamide (3.0 g, 35.7 mmol), 4-*tert*-butylcyclohexanone (5.8 mL, 35.7 mmol), and morpholine (7.1 mL, 71.4 mmol) in EtOH (60.0 mL) was added sulfur (1.1 g, 35.7 mmol) at room temperature. The reaction mixture was stirred at 70 ^{o}C for 12 h. The reaction mixture was cooled to room temperature, diluted with EtOAc and quenched with H_2O. The organic layer was washed with brine, dried over $MgSO_4$, filtered and concentrated. The residue was dissolved in CH_2Cl_2 and collected by adding Et_2O. The resulting solid was collected to afford **8c** (5.2 g, 69%) as a brown solid. ^{1}H NMR (400 MHz, DMSO-d_6) δ 6.91 (s, 1H), 6.48 (brs, 1H), 2.66 (m, 1H), 2.59 (m, 1H), 2.44 (m, 1H), 2.23 (m, 1H), 1.91 (m, 1H), 1.39 (m, 1H), 1.17 (m, 2H), 0.89 (s, 9H); ^{13}C NMR (100 MHz, DMSO-d_6) δ 167.87, 159.34, 129.94, 116.08, 107.08, 44.55, 32.14, 27.10, 26.99, 25.62, 24.18; LRMS (ESI) *m/z* 247 $[M + H]^+$. HRMS (ESI) *m/z* calculated for $C_{13}H_{21}N_2OS^+$ $[M + H]^+$: 253.13. Found: 253.1505.

General procedure A for the synthesis of compounds 7a-c and 9a-i. To a solution of **6** or **8a-c** (1 equiv) in pyridine (0.2 M) was added various acyl chloride (1.1 equiv) at 0 ^{o}C. The reaction mixture was stirred for 1 h at room temperature, quenched with H_2O and diluted with EtOAc. The organic layer was washed with water and brine, dried over $MgSO_4$, filtered and concentrated. The resulting residue was purified by flash column chromatography on silica gel.

2-Pivalamidothiophene-3-carboxamide (7a) Compound **6** (100 mg, 0.70 mmol) was transformed to the target compound using general procedure A. The resulting crude product was purified by flash column chromatography on silica gel (25% EtOAc/hexane) to afford **7a** (108 mg, 84%). ^{1}H NMR (400 MHz, DMSO-d_6) δ 12.65 (s, 1H), 7.94 (brs, 1H), 7.53 (brs, 1H), 7.42 (d, J = 5.8 Hz, 1H), 6.94 (d, J = 5.8 Hz, 1H), 1.23 (s, 1H); ^{13}C NMR (100 MHz, DMSO-d_6) δ 174.76, 167.24, 146.27, 122.94, 115.90, 114.98, 38.56, 30.67, 26.94; LRMS (ESI) *m/z* 183 $[M + H]^+$.

***N*-(3-Carbamoylthiophen-2-yl)furan-2-carboxamide (7b)** Compound **6** (100 mg, 0.70 mmol) was transformed to the target compound using general procedure A. The resulting crude product was purified by flash column chromatography on silica gel (25% EtOAc/hexane) to afford **7b** (122 mg, 82%). ^{1}H NMR (400 MHz, DMSO-d_6) δ 13.12 (s, 1H), 8.03 (dd, J = 1.7, 0.7 Hz, 1H), 8.01 (brs, 1H), 7.60 (brs, 1H), 7.47 (d, J = 5.7 Hz, 1H), 7.32 (dd, J = 3.5, 0.7 Hz, 1H), 7.04 (d, J = 5.7 Hz, 1H), 6.77 (dd, J = 3.5, 1.7 Hz, 1H); ^{13}C NMR (100 MHz, DMSO-d_6) δ 166.98, 153.84, 146.68, 146.09, 145.13, 123.20, 116.64, 116.32, 115.85, 112.97; LRMS (ESI) *m/z* 211 $[M + H]^+$.

2-Benzamidothiophene-3-carboxamide (7c) Compound **6** (100 mg, 0.70 mmol) was transformed o the target compound using general procedure A. The resulting crude product was purified by flash column chromatography on silica gel (25% EtOAc/hexane) to afford **7c** (162 mg, 91%). ^{1}H NMR (400 MHz, DMSO-d_6) δ 13.44 (s, 1H), 8.06 (brs, 1H), 7.93 (m, 2H), 7.64 (m, 4H), 7.50 (d, J = 5.7 Hz, 1H), 7.05 (d, J = 5.7 Hz, 1H); ^{13}C NMR (100 MHz, DMSO-d_6) δ 167.37, 162.46, 146.20, 132.64, 132.13, 129.17, 126.98, 123.17, 116.44, 115.64; LRMS (ESI) *m/z* 253 $[M + H]^+$.

2-Pivalamido-5,6-dihydro-4*H*-cyclopenta[*b*]thiophene-3-carboxamide (9a) Compound **8a** (100 mg, 0.55 mmol) was transformed to the target compound using general procedure A. The resulting crude product was purified by flash column chromatography on silica gel (25% EtOAc/hexane) to afford **9a** (117 mg, 80%). ^{1}H NMR (400 MHz, DMSO-d_6) δ 12.50 (s, 1H), 7.61 (brs, 1H), 6.65 (brs, 1H), 2.90 (t, J = 7.0 Hz, 2H), 2.77 (t, J = 7.2 Hz, 2H), 2.34 (m, 2H), 1.22 (s, 9H); ^{13}C NMR (100 MHz, DMSO-d_6) δ 174.50, 167.50, 149.16, 138.86, 131.33, 110.42, 38.65, 29.03, 28.17, 27.67, 26.94; LRMS (ESI) *m/z* 267 $[M + H]^+$.

2-Pivalamido-5,6,7,8-tetrahydro-4*H*-cyclohepta[*b*]thiophene-3-carboxamide (9b) Compound **8b** (100 mg, 0.48 mmol) was transformed to the target compound using general procedure A. The resulting crude product was purified by flash column chromatography on silica gel (25% EtOAc/hexane) to afford **9b** (121 mg, 86%). ^{1}H NMR (400 MHz, DMSO-d_6) δ 10.42 (s, 1H), 2.67 (m, 4H), 1.81 (m, 2H), 1.58 (m, 4H), 1.23 (s, *9*H); ^{13}C NMR (100 MHz, DMSO-d_6) δ 176.31, 144.52, 135.85, 132.10, 114.75, 98.22, 31.38, 28.35, 28.33, 27.62, 26.92, 26.73; LRMS (ESI) *m/z* 295 $[M + H]^+$. HRMS (ESI) *m/z* calculated for $C_{15}H_{22}N_2NaO_2S^+$ $[M + Na]^+$: 317.13. Found: 317.1227.

6-(*tert*-Butyl)-2-pivalamido-4,5,6,7-tetrahydrobenzo[*b*]thiophene-3-carboxamide (9c) Compound **8c** (100 mg, 0.40 mmol) was transformed to the target compound using general procedure A. The resulting crude product was purified by flash column chromatography on silica gel (25% EtOAc/hexane) to afford **9c** (119 mg, 89%). ^{1}H NMR (400 MHz, DMSO-d_6) δ 12.34 (s, 1H), 7.52 (brs, 1H), 6.86 (brs, 1H), 2.76 (m, 2H), 2.64 (m, 1H), 2.36 (m, 1H), 1.97 (m, 1H), 1.40 (m, 1H), 1.21 (m, 1H), 1.21 (s, 9H), 0.91 (s, 9H); ^{13}C NMR (100 MHz, DMSO-d_6) δ 174.46, 167.87, 144.07, 128.64, 126.28, 114.48, 44.35, 38.56, 32.14, 27.07, 26.94, 26.27, 2540, 24.11; LRMS (ESI) *m/z* 337 $[M + H]^+$. HRMS (ESI) *m/z* calculated for $C_{18}H_{29}N_2O_2S^+$ $[M + H]^+$: 337.19. Found: 337.1890.

***N*-(3-Carbamoyl-5,6-dihydro-4*H*-cyclopenta[*b*]thiophen-2-yl)furan-2-carboxamide (9d)** Compound **8a** (100 mg, 0.55 mmol) was transformed to the target compound using general procedure A. The resulting crude product was purified by flash column chromatography on silica gel (25% EtOAc/hexane) to afford **9d** (144 mg, 95%). ^{1}H NMR (400 MHz, DMSO-d_6) δ 12.95 (s, 1H), 8.02 (d, J = 1.7 Hz, 1H), 7.68 (brs, 1H), 7.29 (d, J = 3.2 Hz, 1H), 6.76 (dd, J = 3.2, 1.7 Hz, 1H), 6.76 (brs, 1H), 2.94 (t, J = 7.2 Hz, 2H), 2.82 (t, J = 7.2 Hz, 2H), 2.37 (m, 2H); ^{13}C NMR (100 MHz, DMSO-d_6) δ 167.22, 153.58, 147.72, 146.51, 146.18, 139.23, 132.22, 116.05, 112.91, 111.40, 29.01, 28.22, 27.68; LRMS (ESI) *m/z* 276 $[M + H]^+$.

***N*-(3-Carbamoyl-5,6,7,8-tetrahydro-4*H*-cyclohepta[*b*]thiophen-2-yl)furan-2-carboxamide (9e)** Compound **8b** (100 mg, 0.48 mmol) was transformed to the target compound using general procedure A. The resulting crude product was purified by flash column chromatography on silica gel (25% EtOAc/hexane) to afford **9e** (129 mg, 89%). ^{1}H NMR (400 MHz, DMSO-d_6) δ 11.54 (s, 1H), 7.98 (d, J = 1.0 Hz, 1H), 7.50 (brs, 2H), 7.27 (d, J = 3.3 Hz, 1H), 6.74 (dd, J = 3.3, 1.0 Hz, 1H), 2.81 (m, 2H), 2.71 (m, 2H), 1.79 (m, 2H), 1.60 (m, 4H); ^{13}C NMR (100 MHz, DMSO-d_6) δ 167.55, 153.74, 146.32,

146.18, 136.91, 134.99, 130.87, 121.06, 115.80, 112.77, 31.46, 28.21, 28.13, 27.48, 27.04; LRMS (ESI) *m/z* 305 $[M + H]^+$.

***N*-(6-(*tert*-Butyl)-3-carbamoyl-4,5,6,7-tetrahydrobenzo[*b*]thiophen-2-yl)furan-2-carboxamide (9f)** Compound **8c** (100 mg, 0.40 mmol) was transformed to the target compound using general procedure A. The resulting crude product was purified by flash column chromatography on silica gel (25% EtOAc/hexane) to afford **9f** (126 mg, 92%). ^{1}H NMR (400 MHz, DMSO-d_6) δ 12.75 (s, 1H), 7.99 (d, *J* = 1.5 Hz, 1H), 7.59 (brs, 1H), 7.28 (d, *J* = 3.3 Hz, 1H), 6.96 (brs, 1H), 6.74 (dd, *J* = 3.3, 1.5 Hz, 1H), 2.79 (m, 2H), 2.68 (m, 1H), 2.39 (m, 1H), 1.97 (m, 1H), 1.42 (m, 1H), 1.23 (m, 1H), 0.90 (s, 9H); ^{13}C NMR (100 MHz, DMSO-d_6) δ 167.57, 153.63, 146.44, 146.26, 142.53, 129.03, 127.26, 115.97, 115.68, 112.86, 44.31, 32.14, 27.04, 26.25, 25.44, 24.02; LRMS (ESI) *m/z* 347 $[M + H]^+$.

2-Benzamido-5,6-dihydro-4*H*-cyclopenta[*b*]thiophene-3-carboxamide (9g) Compound **8a** (100 mg, 0.55 mmol) was transformed to the target compound using general procedure A. The resulting crude product was purified by flash column chromatography on silica gel (25% EtOAc/hexane) to afford **9g** (143 mg, 91%). ^{1}H NMR (400 MHz, DMSO-d_6) δ 13.28 (s, 1H), 7.90 (d, *J* = 7.2 Hz, 2H), 7.65 (m, 4H), 6.78 (brs, 1H), 2.96 (t, *J* = 6.9 Hz, 2H), 2.83 (t, *J* = 7.0 Hz, 2H), 2.37 (m, 2H); ^{13}C NMR (100 MHz, DMSO-d_6) δ 167.59, 162.15, 148.87, 139.23, 132.57, 132.22, 132.04, 129.18, 126.91, 111.16, 29.02, 28.23, 27.70; LRMS (ESI) *m/z* 287 $[M + H]^+$.

2-Benzamido-5,6,7,8-tetrahydro-4*H*-cyclohepta[*b*]thiophene-3-carboxamide (9h) Compound **8b** (100 mg, 0.48 mmol) was transformed to the target compound using general procedure A. The resulting crude product was purified by flash column chromatography on silica gel (25% EtOAc/hexane) to afford **9h** (124 mg, 83%). ^{1}H NMR (400 MHz, DMSO-d_6) δ 11.78 (s, 1H), 7.86 (m, 2H), 7.65 (m, 2H), 7.58 (m, 3H), 2.81 (m, 2H), 2.73 (m, 2H), 1.80 (m, 2H), 1.60 (m, 4H); ^{13}C NMR (100 MHz, DMSO-d_6) δ 167.74, 162.63, 137.82, 135.13, 132.57, 132.33, 130.82, 128.97, 127.03, 121.17, 31.54, 28.28, 28.12, 27.57, 27.13; LRMS (ESI) *m/z* 315 $[M + H]^+$.

2-Benzamido-6-(*tert*-butyl)-4,5,6,7-tetrahydrobenzo[*b*]thiophene-3-carboxamide (9i) Compound **8c** (100 mg, 0.40 mmol) was transformed to the target compound using general procedure A. The resulting crude product was purified by flash column chromatography on silica gel (25% EtOAc/hexane) to afford **9i** (123 mg, 87%). ^{1}H NMR (400 MHz, DMSO-d_6) δ 13.09 (s, 1H), 7.89 (m, 2H), 7.63 (m, 3H), 2.76 (m, 3H), 2.42 (m, 1H), 2.00 (m, 1H), 1.42 (m, 1H), 1.25 (m, 1H), 0.93 (s, 9H);

^{13}C NMR (100 MHz, DMSO-d_6) δ 167.92, 162.24, 143.70, 132.53, 132.35, 129.14, 129.08, 127.07, 126.93, 115.39, 44.35, 32.17, 27.08, 26.29, 25.48, 24.06; LRMS (ESI) *m/z* 357 $[M + H]^+$.

General procedure B for the synthesis of compounds 10a-q. To a solution of ammonium thiocyanate (1.5 equiv) in acetone (0.2 M) was added various acyl chloride (1.0 equiv) at room temperature. The reaction mixture was refluxed for 1 h and then treated with **8a-c** (1.0 equiv). The reaction mixture was allowed to reflux for an additional 1 h and cooled to room temperature and solidified by adding H_2O. The resulting solid was collected and purified by flash column chromatography on silica gel.

2-(3-Benzoylthioureido)-5,6-dihydro-4*H*-cyclopenta[*b*]thiophene-3-carboxamide (10a)
Compound **8a** (100 mg, 0.55 mmol) was transformed to the target compound using general procedure B. The resulting crude product was purified by flash column chromatography on silica gel (5% MeOH/CH_2Cl_2) to afford **10a** (159 mg, 84%). ^{1}H NMR (400 MHz, DMSO-d_6) δ 14.84 (s, 1H), 11.56 (s, 1H), 7.97 (d, *J* = 7.7 Hz, 1H), 7.65 (m, 1H), 7.53 (m, 1H), 7.53 (brs, 1H), 6.89 (brs, 1H), 2.96 (t, *J* = 6.9 Hz, 2H), 2.85 (t, *J* = 7.3 Hz, 2H), 2.36 (m, 2H); ^{13}C NMR (100 MHz, DMSO-d_6) δ 173.41, 166.28, 147.00, 139.64, 133.91, 132.95, 132.15, 128.65, 128.38, 116.40, 29.17, 28.47, 27.62; LRMS (ESI) *m/z* 346 $[M + H]^+$. HRMS (ESI) *m/z* calculated for $C_{16}H_{16}N_3O_2S_2^+$ $[M + H]^+$: 346.06. Found: 346.0614.

2-(3-Benzoylthioureido)-5,6,7,8-tetrahydro-4*H*-cyclohepta[*b*]thiophene-3-carboxamide (10b)
Compound **8b** (100 mg, 0.48 mmol) was transformed to the target compound using general procedure B. The resulting crude product was purified by flash column chromatography on silica gel (5% MeOH/CH_2Cl_2) to afford **10b** (139 mg, 78%). ^{1}H NMR (400 MHz, DMSO-d_6) δ 13.96 (s, 1H), 11.70 (s, 1H), 7.96 (d, *J* = 7.3 Hz, 1H), 7.70 (s, 2H), 7.66 (m, 1H), 7.53 (m, 2H), 2.72 (m, 4H), 1.81 (m, 2H), 1.59 (m, 4H); ^{13}C NMR (100 MHz, DMSO-d_6) δ 173.76, 167.70, 166.50, 134.96, 134.23, 133.15, 132.25, 131.86, 128.69, 128.43, 128.18, 31.78, 28.39, 28.05, 27.78, 27.19; LRMS (ESI) *m/z* 374 $[M + H]^+$.

2-(3-Benzoylthioureido)-6-(*tert*-butyl)-4,5,6,7-tetrahydrobenzo[*b*]thiophene-3-carboxamide (10c)
Compound **8c** (100 mg, 0.40 mmol) was transformed to the target compound using general procedure B. The resulting crude product was purified by flash column chromatography on silica gel (5% MeOH/CH_2Cl_2) to afford **10c** (134 mg, 81%). ^{1}H NMR (400 MHz, DMSO-d_6) δ 14.40 (s, 1H), 11.62

(s, 1H), 7.96 (m, 2H), 7.65 (m, 1H), 7.60 (brs, 1H), 7.53 (m, 2H), 7.25 (brs, 1H), 2.73 (m, 3H), 2.41 (m, 1H), 1.99 (m, 1H), 1.44 (m, 1H), 1.24 (m, 1H), 0.93 (s, 9H); ^{13}C NMR (100 MHz, DMSO-d_6) δ 173.92, 166.87, 166.34, 140.05, 133.04, 132.04, 129.43, 128.80, 128.67, 128.42, 122.35, 44.52, 32.22, 27.10, 25.87, 25.30, 24.08; LRMS (ESI) *m/z* 416 $[M + H]^+$. HRMS (ESI) *m/z* calculated for $C_{21}H_{26}N_3O_2S_2^+$ $[M + H]^+$: 416.14. Found: 416.1385.

***N*-((3-Carbamoyl-5,6-dihydro-4*H*-cyclopenta[*b*]thiophen-2-yl)carbamothioyl)furan-2-carboxamide (10d)** Compound **8a** (100 mg, 0.55 mmol) was transformed to the target compound using general procedure B. The resulting crude product was purified by flash column chromatography on silica gel (5% MeOH/CH_2Cl_2) to afford **10d** (138 mg, 75%). ^{1}H NMR (400 MHz, DMSO-d_6) δ 14.70 (s, 1H), 11.31 (s, 1H), 8.06 (d, *J* = 1.1 Hz, 1H), 7.80 (d, *J* = 3.5 Hz, 1H), 7.57 (brs, 1H), 6.88 (brs, 1H), 6.75 (dd, *J* = 3.5, 1.1 Hz, 1H), 2.95 (t, *J* = 7.0 Hz, 2H), 2.84 (t, *J* = 7.2 Hz, 2H), 2.35 (m, 2H); ^{13}C NMR (100 MHz, DMSO-d_6) δ 172.90, 166.27, 155.80, 148.18, 147.06, 144.77, 139.62, 133.93, 118.37, 116.33, 112.59, 29.20, 28.47, 27.61; LRMS (ESI) *m/z* 336 $[M + H]^+$.

***N*-((3-Carbamoyl-5,6,7,8-tetrahydro-4*H*-cyclohepta[*b*]thiophen-2-yl)carbamothioyl)furan-2-carboxamide (10e)** Compound **8b** (100 mg, 0.48 mmol) was transformed to the target compound using general procedure B. The resulting crude product was purified by flash column chromatography on silica gel (5% MeOH/CH_2Cl_2) to afford **10e** (128 mg, 74%). ^{1}H NMR (400 MHz, DMSO-d_6) δ 13.75 (s, 1H), 11.47 (s, 1H), 8.08 (d, *J* = 1.7 Hz, 1H), 7.83 (d, *J* = 3.7 Hz, 1H), 7.69 (brs, 2H), 6.76 (dd, *J* = 3.7, 1.7 Hz, 1H), 2.70 (m, 4H), 1.81 (m, 2H), 1.59 (m, 4H); ^{13}C NMR (100 MHz, DMSO-d_6) δ 173.41, 166.39, 157.17, 148.49, 144.49, 135.04, 134.18, 132.29, 127.33, 118.73, 112.70, 31.79, 28.39, 28.02, 27.78, 27.19; LRMS (ESI) *m/z* 364 $[M + H]^+$.

***N*-((6-(*tert*-Butyl)-3-carbamoyl-4,5,6,7-tetrahydrobenzo[*b*]thiophen-2-yl)carbamothioyl)furan-2-carboxamide (10f)** Compound **8c** (100 mg, 0.40 mmol) was transformed to the target compound using general procedure B. The resulting crude product was purified by flash column chromatography on silica gel (5% MeOH/CH_2Cl_2) to afford **10f** (142 mg, 88%). ^{1}H NMR (400 MHz, DMSO-d_6) δ 14.23 (s, 1H), 11.35 (s, 1H), 8.06 (d, *J* = 1.7 Hz, 1H), 7.80 (d, *J* = 3.5 Hz, 1H), 7.57 (brs, 1H), 7.24 (brs, 1H), 6.75 (dd, *J* = 3.5, 1.7 Hz, 1H), 2.70 (m, 3H), 2.39 (m, 1H), 1.99 (m, 1H), 1.43 (m, 1H), 1.23 (m, 1H), 0.92 (s, 9H); ^{13}C NMR (100 MHz, DMSO-d_6) δ 173.46, 166.26, 156.35, 148.30, 144.65, 140.04, 129.45, 128.78, 122.31, 118.52, 112.63, 44.51, 32.20, 27.08, 25.86, 25.28, 24.06; LRMS (ESI) *m/z* 406 $[M + H]^+$.

***N*-((3-Carbamoyl-5,6-dihydro-4*H*-cyclopenta[*b*]thiophen-2-yl)carbamothioyl)-4-methylthiazole-5-carboxamide (10g)** Compound **8a** (100 mg, 0.55 mmol) was transformed to the target compound using general procedure B. The resulting crude product was purified by flash column chromatography on silica gel (5% MeOH/CH_2Cl_2) to afford **10g** (153 mg, 76%). ^{1}H NMR (400 MHz, DMSO-d_6) δ 14.69 (s, 1H), 11.57 (s, 1H), 9.20 (s, 1H), 7.60 (brs, 1H), 6.88 (brs, 1H), 2.96 (t, *J* = 6.6 Hz, 2H), 2.84 (t, *J* = 6.7 Hz, 2H), 2.62 (s, 3H), 2.35 (m, 2H); ^{13}C NMR (100 MHz, DMSO-d_6) δ 172.69, 166.36, 160.72, 157.79, 156.43, 147.10, 139.65, 134.00, 124.38, 116.24, 29.17, 28.47, 27.62, 17.24; LRMS (ESI) *m/z* 367 $[M + H]^+$.

2-(3-(3,4-Dimethoxybenzoyl)thioureido)-5,6-dihydro-4*H*-cyclopenta[*b*]thiophene-3-carboxamide (10h) Compound **8a** (100 mg, 0.55 mmol) was transformed to the target compound using general procedure B. The resulting crude product was purified by flash column chromatography on silica gel (5% MeOH/CH_2Cl_2) to afford **10h** (180 mg, 81%). ^{1}H NMR (400 MHz, DMSO-d_6) δ 14.87 (s, 1H), 11.43 (s, 1H), 7.69 (dd, *J* = 8.4, 1.8 Hz, 1H), 7.60 (d, *J* = 1.8 Hz, 1H), 7.51 (brs, 1H), 7.09 (d, *J* = 8.4 Hz, 1H), 6.90 (brs, 1H), 3.86 (s, 3H), 3.85 (s, 3H), 2.95 (t, *J* = 7.0 Hz, 2H), 2.84 (t, *J* = 7.2 Hz, 2H), 2.35 (m, 2H); ^{13}C NMR (100 MHz, DMSO-d_6) δ 173.63, 166.25, 165.44, 152.91, 148.20, 146.98, 139.64, 133.85, 123.67, 122.86, 116.44, 111.54, 110.94, 55.74, 55.67, 29.18, 28.48, 27.62; LRMS (ESI) *m/z* 406 $[M + H]^+$.

2-(3-(3,5-Dimethoxybenzoyl)thioureido)-5,6-dihydro-4*H*-cyclopenta[*b*]thiophene-3-carboxamide (10i) Compound **8a** (100 mg, 0.55 mmol) was transformed to the target compound using general procedure B. The resulting crude product was purified by flash column chromatography on silica gel (5% MeOH/CH_2Cl_2) to afford **10i** (185 mg, 83%). ^{1}H NMR (400 MHz, DMSO-d_6) δ 14.86 (s, 1H), 11.56 (s, 1H), 7.55 (brs, 1H), 7.15 (s, 1H), 6.89 (brs, 1H), 6.75 (s, 1H), 3.83 (s, 6H), 2.96 (t, *J* = 7.0 Hz, 2H), 2.85 (t, *J* = 7.0 Hz, 2H), 2.35 (m, 2H); ^{13}C NMR (100 MHz, DMSO-d_6) δ 173.30, 166.30, 165.70, 160.24, 147.03, 139.65, 133.96, 116.40, 106.27, 105.41, 55.60, 29.20, 28.49, 27.64; LRMS (ESI) *m/z* 406 $[M + H]^+$.

2-(3-(3,4,5-Trimethoxybenzoyl)thioureido)-5,6-dihydro-4*H*-cyclopenta[*b*]thiophene-3-carboxamide (10j) Compound **8a** (100 mg, 0.55 mmol) was transformed to the target compound using general procedure B. The resulting crude product was purified by flash column chromatography on silica gel (5% MeOH/CH_2Cl_2) to afford **10j** (187 mg, 78%). ^{1}H NMR (400 MHz, DMSO-d_6) δ

14.90 (s, 1H), 11.57 (s, 1H), 7.53 (brs, 1H), 7.36 (s, 2H), 6.91 (brs, 1H), 3.88 (s, 6H), 3.75 (s, 3H), 2.96 (t, *J* = 7.5 Hz, 2H), 2.85 (t, *J* = 7.5 Hz, 2H), 2.35 (m, 2H); ^{13}C NMR (100 MHz, DMSO-d_6) δ 173.46, 166.28, 165.38, 152.56, 146.96, 141.53, 139.67, 133.95, 126.66, 116.48, 106.32, 60.15, 56.16, 29.19, 28.50, 27.64; LRMS (ESI) *m/z* 436 $[M + H]^+$.

***N*-((3-Carbamoyl-5,6-dihydro-4*H*-cyclopenta[*b*]thiophen-2-yl)carbamothioyl)benzo[*d*][1,3]dioxole-5-carboxamide (10k)** Compound **8a** (100 mg, 0.55 mmol) was transformed to the target compound using general procedure B. The resulting crude product was purified by flash column chromatography on silica gel (5% MeOH/CH_2Cl_2) to afford **10k** (184 mg, 86%). ^{1}H NMR (400 MHz, DMSO-d_6) δ 14.82 (s, 1H), 11.36 (s, 1H), 7.63 (d, *J* = 8.3 Hz, 1H), 7.53 (s, 1H), 7.53 (brs, 1H), 7.05 (d, *J* = 8.3 Hz, 1H), 6.88 (brs, 1H), 6.15 (s, 2H), 2.95 (t, *J* = 6.8 Hz, 2H), 2.84 (t, *J* = 6.7 Hz, 2H), 2.34 (m, 2H); ^{13}C NMR (100 MHz, DMSO-d_6) δ 173.46, 166.28, 165.13, 151.39, 147.42, 147.02, 139.63, 133.85, 125.60, 124.72, 116.37, 108.42, 107.99, 102.14, 29.18, 28.48, 27.62; LRMS (ESI) *m/z* 390 $[M + H]^+$.

***N*-((3-Carbamoyl-5,6-dihydro-4*H*-cyclopenta[*b*]thiophen-2-yl)carbamothioyl)-2,3-dihydrobenzo[*b*][1,4]dioxine-6-carboxamide (10l)** Compound **8a** (100 mg, 0.55 mmol) was transformed to the target compound using general procedure B. The resulting crude product was purified by flash column chromatography on silica gel (5% MeOH/CH_2Cl_2) to afford **10l** (164 mg, 74%). ^{1}H NMR (400 MHz, DMSO-d_6) δ 14.81 (s, 1H), 11.35 (s, 1H), 7.55 (s, 1H), 7.54 (d, *J* = 9.0 Hz, 1H), 7.54 (brs, 1H), 6.98 (d, *J* = 9.0 Hz, 1H), 6.89 (brs, 1H), 4.32 (m, 4H), 2.95 (t, *J* = 6.9 Hz, 2H), 2.84 (t, *J* = 7.1 Hz, 2H), 2.35 (m, 2H); ^{13}C NMR (100 MHz, DMSO-d_6) δ 173.49, 166.25, 165.15, 147.75, 146.98, 142.98, 139.62, 133.82, 124.61, 122.52, 117.81, 116.95, 116.39, 64.52, 63.93, 29.16, 28.47, 27.61; LRMS (ESI) *m/z* 404 $[M + H]^+$.

2-(3-(3-(Trifluoromethyl)benzoyl)thioureido)-5,6-dihydro-4*H*-cyclopenta[*b*]thiophene-3-carboxamide (10m) Compound **8a** (100 mg, 0.55 mmol) was transformed to the target compound using general procedure B. The resulting crude product was purified by flash column chromatography on silica gel (5% MeOH/CH_2Cl_2) to afford **10m** (157 mg, 69%). ^{1}H NMR (400 MHz, DMSO-d_6) δ 14.88 (s, 1H), 11.93 (s, 1H), 8.32 (s, 1H), 8.23 (d, *J* = 7.9 Hz, 1H), 8.01 (d, *J* = 7.9 Hz, 1H), 7.77 (dd, *J* = 7.9 Hz, 1H), 7.57 (brs, 1H), 6.90 (brs, 1H), 2.97 (t, *J* = 7.2 Hz, 2H), 2.85 (t, *J* = 7.2 Hz, 2H), 2.36 (m, 2H); ^{13}C NMR (100 MHz, DMSO-d_6) δ 173.19, 166.32, 164.99, 147.04, 139.66, 134.02, 133.27,

132.82, 129.61, 129.26, 129.15, 128.83, 125.52, 125.19, 122.49, 116.38, 29.20, 28.48, 27.63; LRMS (ESI) *m/z* 414 $[M + H]^+$.

2-(3-(4-(Trifluoromethyl)benzoyl)thioureido)-5,6-dihydro-4*H*-cyclopenta[*b*]thiophene-3-carboxamide (10n) Compound **8a** (100 mg, 0.55 mmol) was transformed to the target compound using general procedure B. The resulting crude product was purified by flash column chromatography on silica gel (5% MeOH/CH_2Cl_2) to afford **10n** (148 mg, 65%). ^{1}H NMR (400 MHz, DMSO-d_6) δ 14.85 (s, 1H), 11.86 (s, 1H), 8.13 (d, *J* = 8.2 Hz, 2H), 7.90 (d, *J* = 8.2 Hz, 2H), 7.58 (brs, 1H), 6.89 (brs, 1H), 2.96 (t, *J* = 7.2 Hz, 2H), 2.85 (t, *J* = 7.2 Hz, 2H), 2.36 (m, *J* = 7.2 Hz, 2H); ^{13}C NMR (100 MHz, DMSO-d_6) δ 173.09, 166.31, 165.31, 146.98, 139.67, 136326, 134.03, 129.62, 125.26, 125.22, 116.41, 29.17, 28.47, 27.62; LRMS (ESI) *m/z* 414 $[M + H]^+$.

2-(3-(2-Chlorobenzoyl)thioureido)-5,6-dihydro-4*H*-cyclopenta[*b*]thiophene-3-carboxamide (10o) Compound **8a** (100 mg, 0.55 mmol) was transformed to the target compound using general procedure B. The resulting crude product was purified by flash column chromatography on silica gel (5% MeOH/CH_2Cl_2) to afford **10o** (158 mg, 76%). ^{1}H NMR (400 MHz, DMSO-d_6) δ 14.77 (s, 1H), 11.98 (s, 1H), 7.62 (m, 1H), 7.61 (brs, 1H), 7.54 (m, 2H), 7.44 (m, 1H), 6.88 (brs, 1H), 2.97 (t, *J* = 7.0 Hz, 2H), 2.85 (t, *J* = 7.2 Hz, 2H), 2.36 (m, 2H); ^{13}C NMR (100 MHz, DMSO-d_6) δ 172.80, 166.33, 165.55, 147.07, 139.59, 134.50, 134.02, 131.95, 130.04, 129.51, 129.30, 127.08, 116.27, 29.18, 28.47, 27.62; LRMS (ESI) *m/z* 380 $[M + H]^+$. HRMS (ESI) *m/z* calculated for $C_{16}H_{15}ClN_3O_2S_2^+$ $[M + H]^+$: 380.02. Found: 380.0217.

2-(3-(3-Chlorobenzoyl)thioureido)-5,6-dihydro-4*H*-cyclopenta[*b*]thiophene-3-carboxamide (10p) Compound **8a** (100 mg, 0.55 mmol) was transformed to the target compound using general procedure B. The resulting crude product was purified by flash column chromatography on silica gel (5% MeOH/CH_2Cl_2) to afford **10p** (148 mg, 71%). ^{1}H NMR (400 MHz, DMSO-d_6) δ 14.83 (s, 1H), 11.74 (s, 1H), 8.02 (s, 1H), 7.90 (d, *J* = 7.8 Hz, 1H), 7.71 (d, *J* = 8.9 Hz, 1H), 7.57 (brs, 1H), 7.56 (dd, *J* = 8.9, 7.8 Hz, 1H), 6.90 (brs, 1H), 2.96 (t, *J* = 7.3 Hz, 2H), 2.85 (t, *J* = 7.2 Hz, 2H), 2.36 (m, 2H); ^{13}C NMR (100 MHz, DMSO-d_6) δ 173.14, 166.30, 164.93, 147.06, 139.63, 134.24, 133.97, 133.08, 132.59, 130.28, 128.47, 127.40, 116.33, 29.19, 28.48, 27.62; LRMS (ESI) *m/z* 380 $[M + H]^+$.

2-(3-(4-Chlorobenzoyl)thioureido)-5,6-dihydro-4*H*-cyclopenta[*b*]thiophene-3-carboxamide (10q) Compound **8a** (100 mg, 0.55 mmol) was transformed to the target compound using general procedure

B. The resulting crude product was purified by flash column chromatography on silica gel (5% MeOH/CH_2Cl_2) to afford **10q** (165 mg, 79%). ^{1}H NMR (400 MHz, DMSO-d_6) δ 14.83 (s, 1H), 11.69 (s, 1H), 7.97 (d, *J* = 8.6 Hz, 1H), 7.60 (d, *J* = 8.6 Hz, 1H), 7.60 (brs, 1H), 6.89 (brs, 1H), 2.96 (t, *J* = 7.3 Hz, 2H), 2.85 (t, *J* = 7.1 Hz, 2H), 2.35 (m, 2H); ^{13}C NMR (100 MHz, DMSO-d_6) δ 173.24, 166.29, 165.28, 147.02, 139.64, 137.83, 133.94, 131.01, 130.65, 128.44, 116.36, 29.18, 28.48, 27.62; LRMS (ESI) *m/z* 380 $[M + H]^+$. HRMS (ESI) *m/z* calculated for $C_{16}H_{15}ClN_3O_2S_2^+$ $[M + H]^+$: 380.02. Found: 380.0215.

5. Bioassays

CaCCinh-A01 (**1**), T16Ainh-A01 (**2**) and Ani-9 (**3**) were purchased from Sigma-Aldrich. MG132 was purchased from selleckchem. The ANO1 inhibitor, 10bm (**4**) was synthesized as described in previous paper[24].

5.1. Cell culture

U251 and U138 cells kindly provided by Professor Jae-Yong Park (Korea University, Seoul) were cultured at DMEM. U87MG cells purchased from KCLB (Seoul, Korea) were cultured at MEM media, respectively, supplemented with 10% (v/v) fetal bovine serum (FBS), penicillin (100 U/mL) and streptomycin (100 μg/mL) in a humidified 5% CO_2 incubator at 37 °C.

5.2. Isolation of mouse primary astrocyte

The isolation of mouse primary astrocyte was carried out by methods previously reported [40].

5.3. Anti-cell proliferation assay

5.0×10^3 cells per well were seeded in a 96-well plate. After overnight, the test compounds were added to the wells with 1:4 serial dilution in DMSO. After 72 h, the cellular viability was determined by Cell Titer-Glo reagent (G7572, Promega, USA). Dose-response curve was fitted and GI_{50} values were calculated using Graphpad prism 6.0 software. All assays were performed in triplicate, and standard deviation (SD) was determined from three independent experiments.

5.3. ANO1 channel activity assay

5.3.1. ANO1 channel activity assay (fluorescence method) Human ANO1 expressed HEK293 cells were trypsinized, counted and seeded in black, clear-bottomed 96 well plates at a density of 50,000 cells per well and incubated overnight. Next day, media was removed from cell plates and 25 μL assay buffer (1.11 mM $CaCl_2$, 0.43 mM $MgCl_2 \cdot 6H_2O$, 0.36 mM $MgSO_4 \cdot 7H_2O$, 4.98 mM KCl, 0.39 mM KH_2PO_4, 122 mM NaCl, 0.3 mM Na_2HPO_4, 4.86 mM D-glucose, 17.7 mM HEPES, pH 7.4) was

added. FLIPR Red membrane potential dye solution (10Al) was added to the wells and incubated at room temperature for 40-60 min. Dye solution was made up in assay buffer. Compound dilutions (including serial dilutions) were performed in DMSO then transferred to intermediate dilutions within 10 minutes just before adding to the cell plate. Compounds were incubated for 10 minutes at room temperature. The plates were then placed in the FLIPR and fluorescence monitored. After 20 seconds agonist, ionomycin, was added and the fluorescence was monitored for 90 seconds at 488 nm/510-570 nm, ex/em. The compounds and all controls were tested in a final DMSO concentration of 0.5%. Compounds were tested at 30, 10, 3, 1, 0.1, 0.01, and 0.001 μM in duplicate.

5.3.2. Electrophysiological recording (Patch clamp)

Current-voltage (I-V) relationship curves were obtained from HEK293 cells transfected with GFP-mANO1, GFP-mANO2 or GFP-mTTYH1, and U251 cells for endogenous ANO1 currents. Currents were measured by applying 1s duration voltage ramps from +80 to −80 mV (a holding potential of − 10 mV) at room temperature. For measuring ANO1- and ANO2-mediated currents, recording electrodes (4–7 MΩ) were filled with 146 mM CsCl, 5 mM Ca-EGTA-NMDG, 8 mM HEPES, 2 mM $MgCl_2$, and 10 mM sucrose (pH adjusted to 7.3 with CsOH). The standard bath solution contained 139 mM NaCl, 10 mM HEPES, 3 mM KCl, 2 mM $CaCl_2$, 2 mM $MgCl_2$, and 5.5 mM glucose (pH adjusted to 7.3 with NaOH). For measuring TTYH1-mediated currents, the standard solution for pipette contained 70 mM Tris-base, 70 mM aspartic acid, 15 mM HEPES, 0.4 mM $CaCl_2$, 1 mM $MgCl_2$, 1 mM EGTA, 1 mM ATP, and 0.5 mM GTP (pH adjusted to 7.2 with CsOH). Bath contained 70 mM Tris-HCl, 1.5 mM $CaCl_2$, 10 mM HEPES, 10 mM D-glucose and 10 mM sucrose (290 mOsm/kg; pH 7.4 with CsOH). To inhibit K^+ channels, 5 mM triethylamine and 5 mM $BaCl_2$ were added in the bath solution. Hypotonic solutions had the same ionic composition without sucrose from the bath solution (220 mOsm/kg; pH 7.4 with CsOH), and these solutions refereed to a previous study (1). To examine the reversibility of ANO1 current, ANO1 inhibitors were washed out after the maximized inhibition of ANO1 currents were obtained by 10 μM **9c** and **10q**. Whole-cell currents were amplified using the Axopatch 200A patch clamp system (Molecular Devices, USA). Data acquisition was controlled by pCLAMP 10.2 software (Molecular Devices, USA).

5.4. Migration assay (Wound healing method)

U251 cells were seeded in 24-well plates (Thermo Fisher Scientific, MA, USA) at a density of 2.0×10^5 cells per well, and incubated overnight. After 24 h, cells were scraped with a SPLScarTM Scratcher (SPL Life Sciences, ROK) and washed with PBS twice to remove the detached cells and then incubated in complete media. Cells were incubated with various concentrations (1, 5 and 10 μM) of **9c** or **10q** for 18 h. The images of scratched regions were

recorded before and after 18 h incubation, and migration ratios were calculated from migration areas determined using Image J software.

5.5. Invasion assay (Boyden chamber method)

The invasion assay was performed using CHEMICON QCM 24-well Invasion assay kit (ECM 554, Chemicon International, MA, USA). U251 cells were seeded in the 8-μm ECMatrix™-coated transwell chamber (Chemicon International, MA, USA) at a density of 2.5×10^5 cells per well after serum starvation for 24 h. The cells were incubated for 48 h at 37 °C in a humidified 5% CO_2 incubator. Invaded cells from the bottom of the chamber were detached using 225 μL of cell detachment solution (Chemicon International, MA, USA) for 30 min at 37 °C. The detached cells were lysed with 75 μL of lysis buffer (Chemicon International, MA, USA) containing CyQuant GR Dye solution (Chemicon International, MA, USA) for 15 min at room temperature and the fluorescence intensities of 200 μL of the mixtures in a 96-well black-wall plate were measured using a FlexStation3 microplate reader (excitation wavelength of 480 nm and emission wavelength of 520 nm). Invasion ratios were calculated from relative fluorescence intensities acquired at different concentrations (1 and 10 μM) of **9c** or **10q**.

5.6. Western blot assay

E-cadherin antibodies were purchased from cell signaling. ANO1 and β-actin were purchased from SantaCruz. Cells (5×10^5 cells) were treated with indicated compounds for 18 h and briefly washed with ice-cold PBS twice. Cells were then subjected to lysis in a NP40 buffer (50 mM Tris-HCl pH7.5, 1% NP40, 1 mM EDTA, 150 mM NaCl, 5 mM Na_3VO_4 and 2.5 mM NaF) containing 1× protease inhibitor cocktail (Roche). 25 μg/well of lysate was separated by SDS-PAGE gel and transferred to nitrocellulose membrane. All of primary antibodies were pre-diluted in TBS-T at 1:1000 (v/v) except for actin (1:10000), while secondary antibodies were pre-diluted in TBS-T with 1% skim milk at 1:10000.

5.7. Proteosomal degradation analysis of ANO1

The effects of **1, 9c** and **10q** on ANO1 protein level were investigated by western blot analysis. β-actin was used as a loading control. U251 cells (5×10^5 cells) were incubated with 10 μM concentration of the ANO1 inhibitors (**1, 9c** or **10q**) for 24 h. In order to examine the effect of MG132, a proteasome inhibitor, U251 cells (5×10^5 cells) were incubated with 10 μM concentration of the ANO1 inhibitors (**1, 9c** or **10q**) for 6 h, followed by the treatment of MG132 (20 μM) for an additional 18 h. The remaining procedures of the western blotting are the same as those described above.

5.8. Reverse transcription polymerase chain reaction (RT-PCR) analysis

Total RNA in mammalian cell lines was extracted using TRIZOL (Invitrogen, USA) according to the manufacturer's instructions. Reverse transcription was performed with 2 μg of total RNA using M-MLV reverse transcriptase (Promega, USA). PCR reactions were amplified using AccuPower PCR PreMix (Bioneer, ROK) with complementary DNA. Sequences of primers for RT-PCR reactions were as follows: a forward primer for ANO1; 5'-GAGCCAAAGACATCGGAATCTG-3'; a reverse primer for ANO1; 5'-TGAAGGAGATCACGAAGGCAT-3'; a forward primer for β-actin; 5'-TCCTGTGGCATCCACGAAACT-3'; a reverse primer for β-actin; 5'-GAAGCATTTGCGGTGGACGAT-3'. PCR products were resolved on 1.8% agarose gels and relative mRNA levels were determined by densitometry analysis using Image J software.

5.9. Colony formation assay

U251 cells were seeded on 6-well plates (Thermo, USA) at 1.0×10^3 cells per well. The cells were incubated with the indicated compounds for 2 weeks at 37 °C and 5% CO_2. colonies were stained using crystal violet staining solution (0.005% crystal violet, 1% methanol, 1% formaldehyde in PBS) for 24 h. After staining, colonies were washed with PBS 2 times and 10%(v/v) acetic acid for 30 min and detected the A570 nm using plate reader Envision 2013.

5.10. Anchorage Independent Assay

On the 0.6% bottom agar, cells in the complete media containing 0.3% agar was plated at a density of 2.0×10^3 cells in 6-well plates. The cells were incubated with indicated compounds for 14 days at 37 °C and 5% CO_2. Spheroids were stained using crystal violet staining solution (Sigma-Aldrich) for 24 h. The entire area of each well was photographed without magnification, and the average number and size of colonies in each well were counted using ImageJ software.

5.11. Synergy analysis

Combination index (CI) of temozolomide with each ANO1 channel inhibitor was determined by the Chou-Talalay method using CompuSyn software (CompuSyn, USA) (Chou, 2010; Chou & Talalay, 1984). Cell proliferative assay data were used to evaluate the CI values of temozolomide with each ANO1 channel inhibitor. The CI values defines synergism ($CI < 1$), additive effect ($CI = 1$) and antagonism ($CI > 1$).

5.12. Statistical analysis.

Numerical data are presented as mean ± standard deviation. The significance of data for comparison was evaluated by using one-way ANOVA in Prism ver 6.0 (GraphPad software, Inc., CA, USA). *P< 0.05, **P< 0.01, ***P<0.001 and ****P<0.0001.

ASSOCIATED CONTENT

Supporting Information

AUTHOR INFORMATION

Corresponding Author

*E-mail: tbsim@yuhs.ac, Phone: +82-2-2228-0797

Author Contributions

[1]SeungHye Choi and [1]SeongShick Ryu contributed equally to this work. The manuscript was written through contributions of all authors. All authors have given approval to the final version of the manuscript.

Notes

The authors declare no competing financial interest.

Acknowledgements

This work was supported by a grant (2E29260) from Korea Institute of Science and Technology (KIST), and the KU-KIST Graduate School of Converging Science and Technology Program. This research was also supported by the Candidate Development Program (NRF2016M3A9B5940991) and the Bio-Synergy Research Project (NRF2017M3A9C4092979 to J-YP) from the National Research Foundation in Korea.

ABBREVIATIONS

References

[1] C. Hartzell, I. Putzier, and J. Arreola, Calcium-activated chloride channels. Annu. Rev. Physiol. 67 (2005) 719−758.

[2] X. Jin, S. Shah, X. Du, H. Zhang, N. Gamper, Activation of Ca^{2+}□activated Cl^- channel ANO1 by localized Ca^{2+} signals. J. Physiol. 594 (2016) 19−30.

[3] A. Britschgi, A. Bill, H. Brinkhaus, C. Rothwell, I. Clay, S. Duss, M. Rebhan, P. Raman, C.T. Guy, K. Wetzel, E. George, M.O. Popa, S. Lilley, H. Choudhury, M. Gosling, L. Wang, S. Fitzgerald, J. Borawski, J. Baffoe, M. Labow, L.A. Gaither, M. Bentires-Alj, Calcium-activated chloride channel ANO1 promotes breast cancer progression by activating EGFR and CAMK signaling. Proc. Natl. Acad. Sci. USA 110 (2013) E1026−E1034.

[4] F.A. Hanzu, R. Gasa, N. Bulur, P. Lybaert, R. Gomis, W.J. Malaisse, R. Beauwens, A. Sener, Expression of TMEM16A and SLC4A4 in human pancreatic islets. Cell Death. Dis. 29 (2012) 61−64.

[5] Y. Song, J. Gao, L. Guan, X. Chen, J. Gao, K. Wang, Inhibition of ANO1/TMEM16A induces apoptosis in human prostate carcinoma cells by activating TNF-α signaling. Cell Death. Dis. 9 (2018) 703.

[6] D.A. Bijos, M.J. Drake, B. Vahabi, Anoctamin-1 in the juvenile rat urinary bladder. PLoS One 9 (2014) e106190.

[7] M.K. Kashyap, A. Marimuthu, C.J. Kishore, S. Peri, S. Keerthikumar, T.S. Prasad, R. Mahmood, S. Rao, P. Ranganathan, R.C. Sanjeeviah, M. Vijayakumar, K.V. Kumar, E.A. Montgomery, R.V. Kumar, A. Pandey, Genomewide mRNA profiling of esophageal squamous cell carcinoma for identification of cancer biomarkers. Cancer Biol. Ther. 8 (2009) 36−46.

[8] L. Jia, W. Liu, L. Guan, M. Lu, K. Wang, Inhibition of calcium-activated chloride channel ANO1/TMEM16A suppresses tumor growth invasion in human lung cancer. PLoS One 10 (2015) e0136584.

[9] C. Ayoub, C. Wasylyk, Y. Li, E. Thomas, L. Marisa, A. Robé, M. Roux, J. Abecassis, A. de Reyniès, B. Wasylyk, ANO1 amplification and expression in HNSCC with a high propensity for future distant metastasis and its functions in HNSCC cell lines. Br. J. Cancer, 103 (2010) 715−726.

[10] K. Kunzelmann, J. Ousingsawat, R. Benedetto, I. Cabrita, R. Schreiber. Contribution of Anoctamins to Cell Survival and Cell Death. Cancers (Basel) 11 (2019) 382.

[11] M.E. Berens, A. Giese, "... those left behind." Biology and oncology of invasive glioma cells. Neoplasia, 1 (1999) 208−219.

[12] J. Liu, Y. Liu, Y. Ren, L. Kang, L. Zhang, Transmembrane protein with unknown function 16A overexpression promotes glioma formation through the nuclear factor-kappaB signaling pathway. Mol. Med. Rep. 9 (2014) 1068−1074.

[13] Y.-S. Lee, J.K. Lee, Y. Bae, B.-S. Lee, E. Kim, C.-H. Cho, K. Ryoo, J. Yoo, C.-H. Kim, G.-S. Yi, S.-G. Lee, C.J. Lee, S.S. Kang, E.M. Hwang, J.-Y. Park, Suppression of 14-3-3gamma-mediated surface expression of ANO1 inhibits cancer progression of glioblastoma cells. Sci. Rep. 6 (2016) 26413.

[14] S. Rasche, B. Toetter, J. Adler, A. Tschapek, J. F. Doerner, S. Kurtenbach, H. Hatt, H. Meyer, B. Warscheid, E.M. Neuhaus, Tmem16b is specifically expressed in the cilia of olfactory sensory neurons. Chem. senses. 35 (2010) 239−245.

[15] A.B. Stephan, E.Y. Shum, S. Hirsh, K.D. Cygnar, J. Reisert, H. Zhao, ANO2 is the cilial calcium-activated chloride channel that may mediate olfactory amplification. Proc. Natl. Acad. Sci. USA 106 (2009) 11776−11781.

[16] Y. Zhang, Z. Zhang, S. Xiao, J. Tien, S. Le, T. Le, L.Y. Jan, H. Yang, Inferior olivary TMEM16B mediates cerebellar motor learning. Neuron. 95 (2017) 1103−1111.

[17] F.R.S. Lima, S.A. Kahn, R.C. Soletti, D. Biasoli, T. Alves, A.C.C. Fonseca, C. Garcia, L. Romão, J. Brito, R. Holanda-Afonso, J. Faria, H. Borges, V. Moura-Neto, Glioblastoma: therapeutic challenges, what lies ahead. Biochim. Biophys. Acta.-Reviews on Cancer, 1826 (2012) 338−349.

[18] R. Stupp, W.P. Mason, M.J. Bent, M. Weller, B. Fisher, M.J.B. Taphoorn, K. Belanger, A.A. Brandes, C. Marosi, U. Bogdahn, J. Curschmann, R.C. Janzer, S.K. Ludwin, T. Gorlia, A.

Allgeier, D. Lacombe, J.G. Cairncross, E. Eisenhauer, R.O. Mirimanoff, European Organisation for Research and Treatment of Cancer Brain Tumor and Radiotherapy Groups; National Cancer Institute of Canada Clinical Trials Group Radiotherapy plus concomitant and adjuvant temozolomide for glioblastoma. N. Engl. J. Med., 352 (2005) 987−996.

[19] H.S. Friedman, M.D. Prados, P.Y. Wen, T. Mikkelsen, D. Schiff, L.E. Abrey, W.K. Yung, N. Paleologos, M.K. Nicholas, R. Jensen, J. Vredenburgh, J. Huang, M. Zheng, T. Cloughesy, Bevacizumab alone and in combination with irinotecan in recurrent glioblastoma. J Clin. Oncol., 27 (2009) 4733−4740.

[20] A. Bill, M.L. Hall, J. Borawski, C. Hodgson, J. Jenkins, P. Piechon, O. Popa, C. Rothwell, P. Tranter, S. Tria, T. Wagner, L. Whitehead, L.A. Gaither, Small Molecule-Facilitated Degradation of ANO1 Protein: A New Targeting Approach for Anticancer Therapeutics. J. Biol. Chem. 289 (2014) 11029−11041.

[21] A.J. Davis, J. Shi, H.AT. Pritchard, P.S. Chadha, N. Leblanc, G. Vasilikostas, Z.Yao, AS. Verkman, A.P. Albert, I.A. GreenwoodDavis, Potent vasorelaxant activity of the TMEM16A inhibitor T16A(inh) -A01. Br. J. Pharmacol. 168 (2013) 773−784.

[22] Y. Seo, H.K. Lee, J. Park, D.K. Jeon, S. Jo, M. Jo, W. Namkung, Ani9, a novel potent small-molecule ANO1 inhibitor with negligible effect on ANO2. PLoS One 11 (2016) e0155771.

[23] Y. Seo, J. Kima, J. Chang, S.S. Kim, W. Namkung, I. Kim, Synthesis and biological evaluation of novel Ani9 derivatives as potent and selective ANO1 inhibitors. Eur. J. Med. Chem. 160 (2018) 245−255.

[24] E.C. Truong, P.W. Phuan, A.L. Reggi, L. Ferrera, L.J.V. Galietta, S.E. Levy, A.C. Moises, O. Cil, E. Diez-Cecilia, S. Lee, A.S. Verkman, M.O. Anderson, Substituted 2-Acylaminocycloalkylthiophene-3-carboxylic Acid Arylamides as Inhibitors of the Calcium-Activated Chloride Channel Transmembrane Protein 16A (TMEM16A). J. Med. Chem. 60 (2017) 4626−4635.

[25] K. Gewald, E. Schinke, H. Böttcher, Heterocyclen aus CH□aciden nitrilen, VIII. 2□amino□ thiophene aus methylenaktiven nitrilen, carbonylverbindungen und Schwefel. Chem. Ber. 99 (1966) 94−100.

[26] R.W. Sabnis, The gewald synthesis. Sulfur Rep. 16 (1994) 1−17.

[27] G.A. Eller, W. Holzer, First synthesis of 3-acetyl-2-aminothiophenes using the gewald reaction. Molecules 11 (2006) 371−376.

[28] M. Mahdavi, M.S. Shirazi, R. Taherkhani, M. Saeedi, E. Alipour, F.H. Moghadam, A. Moradi, H. Nadri, S. Emami, L. Firoozpour, A. Shafiee. A. Foroumadi, Synthesis, biological evaluation and docking study of 3-aroyl-1-(4-sulfamoylphenyl) thiourea derivatives as 15-lipoxygenase inhibitors. Eur. J. Med. Chem. 82 (2014) 308−313.

[29] E. Molokanova, A. Savchenko, Bright future of optical assays for ion channel drug discovery. Drug Discov. Today 13 (2008) 14−22.

[30] D.F. Baxter, M. Kirk, A.F. Garcia, A. Raimondi, M.H. Holmqvist, K.K. Flint, D. Bojanic, P.S. Distefano, R. Curitis, Y. Xie, A novel membrane potential-sensitive fluorescent dye improves cell-based assays for ion channels. J. Biomol. Screen 7 (2002) 79−85.

[31] W. Namkung, P.-W. Phuan, A. Verkman, TMEM16A inhibitors reveal TMEM16A as a minor component of calcium-activated chloride channel conductance in airway and intestinal epithelial cells. J. Biol. Chem. 286 (2011) 2365−2374.

[32] M. Abdullah, L. Guruprasad, Structural insights into the inhibitor binding and new inhibitor design to Polo-like kinase-1 Polo-box domain using computational studies. J. Biomol. Struct. Dyn. 37 (2019) 3410−3421.

[33] R.K. Singh, T. Mandal, N. Balsubramanian, T. Viaene, T. Leedahl, N. Sule, G. Cook, D.K. Srivastava, Histone deacetylase activators: N-acetylthioureas serve as highly potent and isozyme selective activators for human histone deacetylase-8 on a fluorescent substrate. Bioorg. Med. Chem. Lett. 21 (2011) 5920−5923.

[34] Z. Liu, S. Zhang, F. Hou, C. Zhang, J. Gao, K. Wang, Inhibition of Ca^{2+}-activated chloride channel ANO1 suppresses ovarian cancer through inactivating PI3K/Akt signaling. Int. J. Cancer 144 (2019) 2215−2226.

[35] L. Guan, Y. Song, J. Gao, J. Gao, K.Wang, Inhibition of calcium-activated chloride channel ANO1 suppresses proliferation and induces apoptosis of epithelium originated cancer cells. Oncotarget 7 (2016) 78619−78630.
[36] J.-Y. Kim, H.Y. Youn, J. Choi, S.K. Baek, S.Y. Kwon, B.K. Eun, J.-Y. Park, K.H. Oh, Anoctamin-1 affects the migration and invasion of anaplastic thyroid carcinoma cells. Anim. Cells Syst. 23 (2019) 294−301.
[37] J.S. Bae, J.Y. Park, S.-H. Park, S.H. Ha, A.R. An, S.J. Noh, K.S. Kwon, S.H. Jung, H.S. Park, M.J. Kang, K.Y. Jang, Expression of ANO1/DOG1 is associated with shorter survival and progression of breast carcinomas. Oncotarget 9 (2018) 607−621.
[38] C.Y. Lee, Strategies of temozolomide in future glioblastoma treatment. Onco. Targets Ther. 10 (2017) 265−270.
[39] M. Karsy, M. Gelbman, P. Shah, O. Balumbu, F. Moy, E. Arslan, Established and emerging variants of glioblastoma multiforme: review of morphological and molecular features. Folia Neuropathol. 50 (2012) 301−321.
[40] S.Schildge, C.Bohrer, K.Beck, C.Schachtrup, Isolation and Culture of Mouse Cortical Astrocytes . J. Vis. Exp. 2013; (71): 50079.

Highlight

- Unique 2-aminothiophene-3-carboxamide derivatives were designed and synthesized.
- ANO1 inhibitory activity from FLIPR assay were confirmed by patch clamp recording.
- **9c** and **10q** strongly inhibit ANO1 channel activity with selectivity over ANO2.
- **9c** and **10q** suppress proliferation, migration and invasion of glioblastoma cells.
- Synergistic effects of combination of TMZ and **9c** in GBM cells were found.

Declaration of interests

☑ The authors declare that they have no known competing financial interests or personal relationships that could have appeared to influence the work reported in this paper.

☐The authors declare the following financial interests/personal relationships which may be considered as potential competing interests: